AGU PUBLICATIONS

Global Biogeochemical Cycles

RESEARCH ARTICLE
10.1002/2015GB005248

Key Points:
- Large decadal increase in the uptake of anthropogenic carbon in the North Atlantic
- The pH in the surface waters has decreased by 0.0021 ± 0.0007 per year
- Eddies significantly impact anthropogenic carbon inventories

Supporting Information:
- Texts S1 and S2 and Figure S1
- Table S1

Correspondence to:
F. J. Millero,
fmillero@rsmas.miami.edu

Citation:
Woosley, R. J., F. J. Millero, and R. Wanninkhof (2016), Rapid anthropogenic changes in CO_2 and pH in the Atlantic Ocean: 2003–2014, *Global Biogeochem. Cycles*, *30*, 70–90, doi:10.1002/2015GB005248.

Received 23 JUL 2015
Accepted 2 JAN 2016
Accepted article online 6 JAN 2016
Published online 30 JAN 2016

Rapid anthropogenic changes in CO_2 and pH in the Atlantic Ocean: 2003–2014

Ryan J. Woosley[1], Frank J. Millero[1], and Rik Wanninkhof[2]

[1]Rosenstiel School of Marine and Atmospheric Science, University of Miami, Miami, Florida, USA, [2]Ocean Chemistry Division, AOML, NOAA, Miami, Florida, USA

Abstract The extended multilinear regression method is used to determine the uptake and storage of anthropogenic carbon in the Atlantic Ocean based on repeat occupations of four cruises from 1989 to 2014 (A16, A20, A22, and A10), with an emphasis on the 2003–2014 period. The results show a significant increase in basin-wide anthropogenic carbon storage in the North Atlantic, which absorbed 4.4 ± 0.9 Pg C decade^{-1} from 2003 to 2014 compared to 1.9 ± 0.4 Pg C decade^{-1} for the 1989–2003 period. This decadal variability is attributed to changing ventilation patterns associated with the North Atlantic Oscillation and increasing release of anthropogenic carbon into the atmosphere. There are small changes in the uptake rate of CO_2 in the South Atlantic for these time periods (3.7 ± 0.8 Pg C decade^{-1} versus 3.2 ± 0.7 Pg C decade^{-1}). Several eddies are identified containing ~20% more anthropogenic carbon than the surrounding waters in the South Atlantic demonstrating the importance of eddies in transporting anthropogenic carbon. The uptake of carbon results in a decrease in pH of ~0.0021 ± 0.0007 year^{-1} for surface waters during the last 10 years, in line with the atmospheric increase in CO_2.

1. Introduction

In 1989, the annual average concentration of CO_2 in the atmosphere was 355 ppm, by early 2014 it had increased to 397 ppm (Scripps CO_2 program, http://scrippsco2.ucsd.edu/). This rapid nonlinear rise in atmospheric CO_2 is causing a change in the planetary radiation balance and an increase in the average global temperature which is associated with adverse climate change effects [*Stocker et al.*, 2013]. The rise is modulated as a result of the uptake of roughly one half of anthropogenic CO_2 emissions by the oceans and land [*Le Quéré et al.*, 2015]. The uptake by land is generally a result of increased biomass, while the uptake by the oceans is driven by thermodynamics and thermohaline circulation in which the surface ocean remains in (near) equilibrium with the atmosphere by absorbing CO_2 [*Millero*, 2007]. Absorbed CO_2 is then transported to the deep interior ocean through deep and intermediate water formation.

While oceanic uptake of CO_2 helps to slow the increase in the atmosphere and slow climate change, it is not without its own set of problems. When carbon dioxide dissolves in the ocean, most react with water to form carbonic acid (H_2CO_3), which then dissociates into carbonate (CO_3^{2-}) or bicarbonate (HCO_3^-), releasing protons (H^+). The result is an increase in the total inorganic carbon (TCO_2) and a decrease in pH. Decreases in pH and associated changes in TCO_2 are known to have a variety of effects on calcifying organisms and other processes in the oceans. These processes include decreases in calcification [*Gattuso et al.*, 1998; *Kleypas et al.*, 1999; *Langdon et al.*, 2000; *Langdon and Atkinson*, 2005], increases in photosynthesis [*Rost and Riebesell*, 2004; *Palacios and Zimmerman*, 2007; *Zondervan*, 2007], increases in nitrogen fixation [*Barcelos e Ramos et al.*, 2007; *Hutchins et al.*, 2007], decreases in reproduction [*Alvarado-Alvarez et al.*, 1996; *Desrosiers et al.*, 1996; *Kurihara and Shirayama*, 2004; *Michaelidis et al.*, 2005], and changes in metal speciation [*Millero et al.*, 2009] that can lead to increased copper toxicity [*Campbell et al.*, 2014].

Although oceans worldwide take up anthropogenic carbon dioxide, not all areas are impacted equally [*Lee et al.*, 2003; *Sabine et al.*, 2004; *Khatiwala et al.*, 2013]. The Atlantic Ocean is an area of high anthropogenic CO_2 uptake and storage relative to its size as a result of strong meridional overturning circulation and formation of North Atlantic Deep Water (NADW), rather than just air-sea gas transfer [*Sarmiento et al.*, 1992]. This makes the Atlantic unique in the depth in which anthropogenic CO_2 can penetrate over decadal time scales—capable of reaching the bottom (~3000 m) in the far North Atlantic [*Wanninkhof et al.*, 2010], compared to the Pacific, where anthropogenic carbon only penetrates the upper ~1000 m on decadal time scales [*Sabine et al.*, 2008; *Waters et al.*, 2011]. Several studies have quantified the uptake and distribution

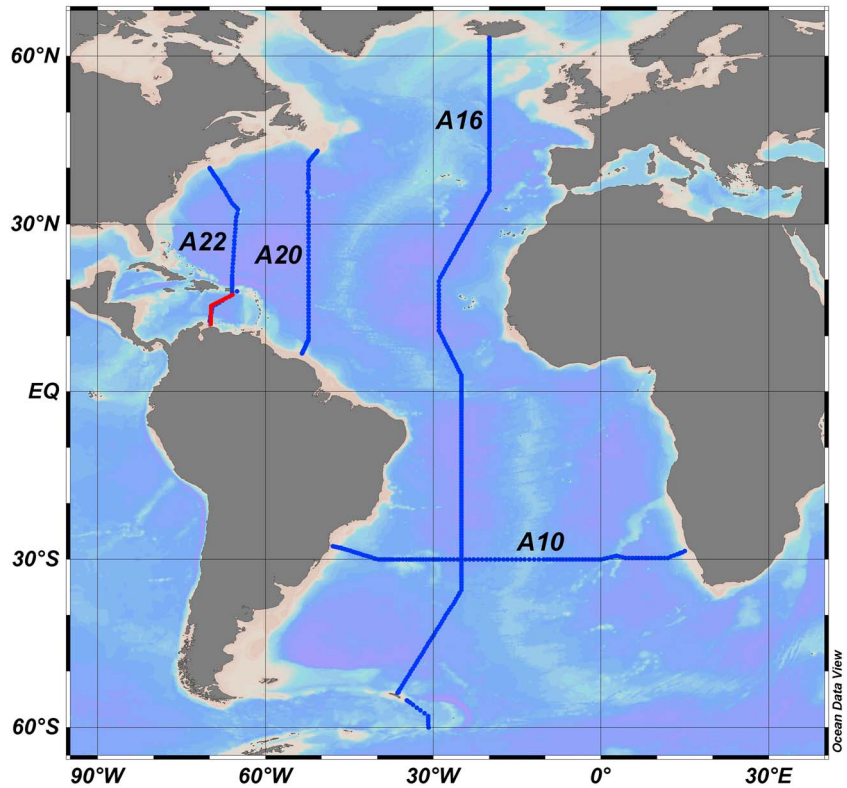

Figure 1. Cruise track for the four sections used in this paper. The section shown in red is not included in the results of this paper.

of anthropogenic carbon over the 1990s into the early 2000s using measurements of the carbon system made over several repeat hydrography cruises (World Ocean Circulation Experiment (WOCE), Ocean Atmosphere Carbon Exchange Study (OACES), South Atlantic Ventilation Experiment (SAVE), Climate Variability CO_2 Repeat Hydrography (CLIVAR), and Global Ocean Ship-Based Hydrographic Investigations Program (GOSHIP)) [*Lee et al.*, 2003; *Sabine et al.*, 2004; *Murata et al.*, 2008; *Wanninkhof et al.*, 2010; *Waters et al.*, 2011] and other methods such as Transient Time Distributions [*Watanabe et al.*, 2000; *Tanhua et al.*, 2006; *Steinfeldt et al.*, 2009]. This study builds on these previous studies by extending the temporal coverage into early 2014 and comparing uptake rates and column inventories of the last two decades.

With 25 years of high-quality carbon data coving the North Atlantic, it is now becoming possible to answer questions about the decadal variability of the uptake and storage of anthropogenic CO_2 in the Atlantic. A growing body of work is showing large variability of the Meridional Overturning Circulation (MOC) [*Pérez et al.*, 2013; *Zhao and Johns*, 2014; *Srokosz and Bryden*, 2015], which plays a large role in the variations of storage rates of anthropogenic CO_2 in the North Atlantic. A slowdown of the MOC would result in a decrease in the ability of the North Atlantic to transport CO_2 from the atmosphere into the interior ocean, but available data have been insufficient to confirm this [*Sabine and Tanhua*, 2010]. Recent work has also demonstrated a strong relationship between the North Atlantic Oscillation (NAO) and uptake rates in the Atlantic [*Pérez et al.*, 2010, 2013] as well as large variability in the anthropogenic CO_2 sink in the tropical North Atlantic [*Zunino et al.*, 2015], indicating that strong decadal variability in the North Atlantic carbon sink. *Wanninkhof et al.* [2010] found a relatively low storage of anthropogenic carbon in the North Atlantic during the 1990s, the additional data from this study puts this in the context of large decadal variability.

2. Data Description and Quality

Four oceanographic sections were analyzed (Figure 1), each of which has been occupied three times over a period of 15–25 years. Three are north-south sections; A20 and A22 cover the western Basin of the North Atlantic, and A16 traverses the Atlantic from Iceland into the Southern Ocean, with coverage of the eastern

Table 1. Cruises Used in This Paper Along With Corrections Made to the Data

Section/Cruise	CDIAC Name	Expocode	Dates[a]	Extent	Nominal Latitude/Longitude	Data Corrections/Notes[b]
			A16			
OACES/SAVE	SAVE 5	318MSAVE5	1–17 Feb 1989	32°S–54°S	25°W	NO_3^-: 0.982
	SAVE6/HYDROS4	318MHYDROS4	21 Mar to 8 Apr 1989	0°S–32°S	25°W	NO_3^-: 0.982
	OACES N.Atl-93	3175 MB93	8 Jul to 30 Aug 1993	64°N–5°S	20°W	O_2: +7.5 μmol kg^{-1}; NO_3^-: 0.996
CLIVAR	CLIVAR A16N	33RO200306	19 Jun to 9 Aug 2003	64°N–6°S	20°W	--
	CLIVAR A16S	33RO200501	17 Jan to 21 Feb 2005	2°S–60°S	25°W	--
GOSHIP	GOSHIP A16N	33RO20130803	3 Aug to 3 Oct 2013	63°N–6°S	20°W	--
	GOSHIP A16S	33RO20131223	23 Dec 2013 to 4 Feb 2014	6°S–60°S	25°W	--
			A20			
WOCE	WOCE A20	316N151_3	Jul 17 to 10 Aug 1997	43°N–7°N	52°W	--
CLIVAR	CLIVAR A20	316 N200309	22 Sep to 20 Oct 2003	43°N–7°N	52°W	--
GOSHIP	GOSHIP A20	33AT20120419	19 Apr to 15 May 2012	43°N–6°N	52°W	--
			A22			
WOCE	WOCE A22	316N151_4	15 Aug to 3 Sep 1997	41°N–18.5°N	65°W	Excludes data south of Puerto Rico
CLIVAR	CLIVAR A22	316 N200310	23 Oct to 13 Nov 2003	40°N–18.5°N	65°W	Excludes data south of Puerto Rico pH: −0.010 pH units; PO_4^-: 1.03
GOSHIP	GOSHIP A22	33AT20120324	24 Mar to 17 Apr 2012	40°N–18.5°N	65°W	Excludes data south of Puerto Rico
			A10			
WOCE	WOCE A10	06MT22_5	28 Dec 1992 to 31 Jan 1993	47°W–15°E	30°S	--
CLIVAR	CLIVAR A10	49NZ20031106	6 Nov to 5 Dec 2003	48°W–15°E	30°S	CFC-11: 0.95
GOSHIP	GOSHIP A10	33RO20110926	26 Sep to 31 Oct 2011	48°W–15°E	30°S	--

[a]Dates that ship was occupying stations or in transit.
[b]Numbers with units indicate a constant offset, without units indicates correction factor (ratio). Corrections determined by *Key et al*. [2004] and *Wanninkhof et al*. [2003]. See text for details.

Basin in the north and the western Basin in the south. The fourth is an east-west section, A10, which crosses the South Atlantic (descriptions given in Table 1). Since some cruises were comprised of multiple legs and have been given various names in different papers, the cruise names, as used in this paper, are provided with their official designation (Expocode) for clear identification. Cruises in this paper will be referred to by their section ID (i.e., A16) and program (i.e., CLIVAR) to indicate their location and time of occupation.

The A22 cruise had deviations in track between repeat occupations. The cruise tracks south of Puerto Rico diverged between the different occupations, so these data were not used in our analysis. The A22 WOCE occupation's northern portion diverged from the CLIVAR and GOSHIP occupations. At approximately 33.5°N, the WOCE section continues straight northward toward Canada, while the CLIVAR and GOSHIP occupations head diagonally toward Massachusetts. For this reason, data north of 33.5°N is excluded from our analysis for this WOCE occupation. The GOSHIP/CLIVAR occupations of A22 can be offset by as much as 1° of longitude in some locations, but this difference is small enough to not affect the result.

One of the biggest challenges in quantifying anthropogenic CO_2 is separating natural variability, which requires high-quality data sets and a means to quantify changes in the natural component. When identifying small changes over large time scales, it is important to assess the quality and consistency of the various data sets, particularly for potential artifacts and biases. All cruises followed standard protocols for sampling and analysis [*World Ocean Circulation Experiment*, 1994; *U.S. Department of Energy*, 1994], and certified reference materials were used whenever available. Details on analysis can be found in the comprehensive cruise data reports for each cruise at http://cchdo.ucsd.edu. Several studies have examined the consistency of the older data sets, using comparisons of deep water and regional and crossover comparisons [*Castle et al*., 1998; *Gouretski and Jancke*, 2000; *Wanninkhof et al*., 2003; *Key et al*., 2004, 2010]. Most data were found to be consistent between cruises; however, a few corrections have been made (Table 1). As in *Wanninkhof et al*. [2010], we chose to use the 1989 SAVE 5 and 6 cruises instead of the 1991 OACES cruise for the A16S section because of the higher spatial resolution and the farther southernmost extent (54°S for SAVE and 32°S for OACES).

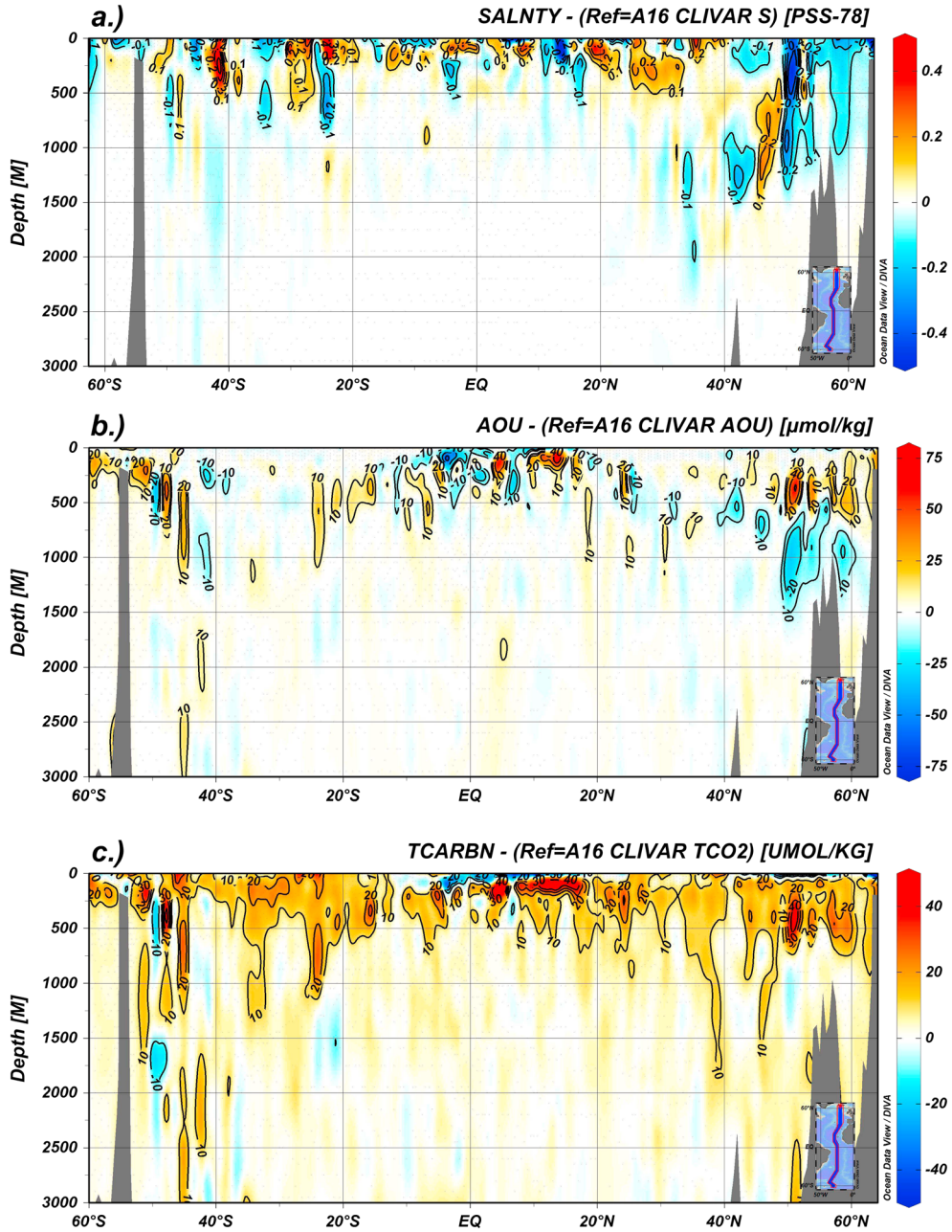

Figure 2. Difference in measured parameters in the upper 3000 m along A16 between GOSHIP and CLIVAR occupations for (a) salinity, (b) AOU, and (c) TCO_2.

South of 32°S there is a decrease in the sampling resolution for all the carbon parameters for SAVE, with the southernmost region having 1 to 3° spacing in the deep waters. TCO_2 has the most data points, with partial pressure of CO_2 (pCO_2) being even more limited. For the SAVE cruises only, total alkalinity (TA) was calculated from TCO_2 and pCO_2. These limitations increase the error and uncertainties for this region in the 1990s, particularly for deep waters, and therefore, waters with a density $\sigma_4 > 45.963$ have been excluded from the SAVE 1989 data.

For the cruises occurring from 2011 to 2014, consistency with older data was determined by comparing deep water data between CLIVAR and GOSHIP occupations and the single crossover point between A16 and A10. For all cruises, waters deeper than 1500 m were compared to the CLIVAR era cruise. To account for differences in total alkalinity (TA) and TCO_2 as a result of changes in salinity, normalized values were compared (NTA = TA/S*35 and $NTCO_2 = TCO_2$/S*35). Values of NTA and $NTCO_2$ in deep waters unaffected by anthropogenic

perturbations or variations in fronts agreed within 1.1 μmol kg^{-1} and 2.4 μmol kg^{-1}, respectively; pH generally agreed within 0.01. No clear bias or pattern was found for any of the cruises. For A16, which consisted of three separate legs, crossover stations were measured between each leg. No significant differences were found for any of the crossover points. The crossover point between A16 and A10 showed no significant differences for TA and TCO_2. Details of the A16 comparisons for pH and TA can be found in *Millero et al*. [2014]. Similar results were found for comparisons of deep water between the A10, A20, and A22 cruises. For A20, there is an area near the surface around 39°N which showed large changes in NTA of ≈ 10–30 μmol kg^{-1}. This has a significant impact on the assumption of constant alkalinity when attributing changes in pH, as discussed in the results.

3. Decadal Changes in Water Properties

Below the winter mixed layer, natural variability of physical and chemical water properties on decadal time scales is largely a result of changes in circulation—heave and movement of fronts, ventilation, and remineralization of organic matter; all of which can affect TCO_2. Before separating out the anthropogenic CO_2 from this natural variability, we look at the total measured changes in the physical and chemical parameters.

Changes in salinity, apparent oxygen utilization (AOU), and TCO_2 along A16 (Figure 2) between the GOSHIP and CLIVAR occupations show that significant changes only occur in the surface and intermediate waters. The majority of the changes in salinity (Figure 2a) occur in the surface. Some decreases are seen in subsurface waters of the far North Atlantic but are generally smaller than the increases observed between the CLIVAR and OACES/SAVE occupations described in *Wanninkhof et al*. [2010]. The changes in AOU (Figure 2b) are mostly confined to the upper 1000 m. In the region north of 40°N, there are areas of increases in the near surface to 700 m range and decreases in the 700–1500 m range, opposite of the pattern seen in the previous decade [*Wanninkhof et al*., 2010]. The changes in TCO_2 (Figure 2c) show a general increase in the upper 1000 m with a range of 10 to 20 μmol kg^{-1}, the approximate decadal change expected from uptake of anthropogenic CO_2. Areas with larger or smaller changes generally correspond to changes in AOU and salinity suggesting natural variability in TCO_2 caused by changes in remineralization and ventilation shifts. Changes in TCO_2 in intermediate waters in the Southern Ocean correspond to changes in Si and are attributed to movement of the subpolar front discussed in more detail in the Appendix A. The total decadal change for the Atlantic (natural plus anthropogenic) determined by integrating the differences in TCO_2 and normalizing to 10 years is 10.6 Pg C decade^{-1}. This value will be compared to the anthropogenic changes determined below.

4. Methods

4.1. Determining Anthropogenic CO_2

Compared to changes in TCO_2, described in the previous section, anthropogenic carbon in the ocean cannot be directly measured. Instead, it must be separated from the natural background processes and variability. Several methods have been developed to do this. The first methods attempted to estimate the increase in TCO_2 attributed to anthropogenic CO_2 invasion since the industrial revolution began (C_{anthro}) [*Brewer*, 1978; *Chen and Millero*, 1979; *Gruber et al*., 1996; *Sabine et al*., 2002]. Newer methods were developed to calculate the amount of anthropogenic carbon between two repeat cruises (ΔC_{anthro}), which can be useful in determining decadal variability and changes in uptake over time.

The extended multilinear regression (eMLR) technique developed by *Friis et al*. [2005], which expanded on the MLR approach [*Wallace*, 1995], has been widely used to detect changes in anthropogenic carbon uptake throughout the major oceans over time [*Friis et al*., 2005; *Sabine et al*., 2008; *Brown et al*., 2010; *Wanninkhof et al*., 2010; *Waters et al*., 2011]. This method removes natural variability as a result of changes in biological production, calcium carbonate production/dissolution, and circulation without relying on assumptions of Redfield ratios, preformed total alkalinity, or (dis)equilibrium with the atmosphere that other methods rely on. The eMLR is applied along isopycnal surfaces since this is the predominant pathway for anthropogenic CO_2 to penetrate into the interior ocean [*Gruber et al*., 1996; *Quay et al*., 2007]. Applying the method along isopycnals also helps to account for variability caused by vertical heave [*Doney et al*., 2007; *Levine et al*., 2008] and allows one to apply the eMLR all the way to the surface instead of extrapolating from below the winter mixed layer, when cruises are performed during the same season and surface water conditions are

similar [*Wanninkhof et al.*, 2010]. The eMLR also shows lower residuals in areas of large TCO_2 gradients (typically 500–1500 m) that are common in single MLR fits [*Brown et al.*, 2010].

The eMLR technique is purely statistical and fits physical (T, S, etc.) and biogeochemical (AOU, nutrients, etc.) parameters to linear equations under the assumption that natural variability in TCO_2 are linearly related to these physical and biogeochemical parameters, while anthropogenic changes are not. The TCO_2 of the first occupation of a section is fit to a multilinear regression using independent physical and chemical properties for a given isopycnal surface as shown by

$$TCO_{2,MLR1,t1} = a_1 + b_1\,S_{t1} + \ c_1T_{t1} + \ d_1AOU_{t1} + e_1TA_{t1} + f_1NO_{3,t1} \tag{1}$$

where subscripts 1 and $t1$ indicate the first fit at time 1. A second MLR is then fit to the second occupation, using the same parameters with subscripts 2 and $t2$ indicating the second occupation:

$$TCO_{2,MLR2,t2} = a_2 + b_2S_{t2} + c_2T_{t2} + d_2AOU_{t2} + e_2TA_{t2} + f_2NO_{3,t2} \tag{2}$$

The change in TCO_2 is then calculated by subtracting the coefficients from the two fits and using the values of the parameters at $t2$:

$$\begin{aligned}\Delta TCO_{2,eMLR} = TCO_{2,MLR2,t2} - TCO_{2,MLR1,t1} = (a_2 - a_1) + (b_2 - b_1)\ S_{t2} + (c_2 - c_1)\ T_{t2} + \\ (d_2 - d_1)\ AOU_{t2} + (e_2 - e_1)\ TA_{t2} + (f_2 - f_1)\ NO_{3,t2}\end{aligned} \tag{3}$$

The value of $\Delta TCO_{2,eMLR}$ is equal to the change in anthropogenic carbon (ΔC_{anthro}) in the ocean during that time period. There are some caveats to the eMLR technique that should be noted. It assumes that the independent variables are not cross correlated, while in reality there is considerable cross correlation among them [*Thacker*, 2012]. This can influence which parameters are most important and can lead to overfitting. The relationships between TCO_2 and the independent variables are also not entirely linear over the full oceanic range. We address this nonlinearity by separating the eMLR into density surfaces. Separating the fits by density surface addresses many of the issues with the eMLR and can likely explain some of the biases found in the model results of *Levine et al.* [2008], which used a single eMLR for the entire depth range. Detailed critiques of the eMLR method are given in *Levine et al.* [2008], *Thacker* [2012], and *Plancherel et al.* [2013]. Issues specific to data used here are also discussed in Appendix A.

The parameters used in the fit are not universal, and the best choice of parameters varies by geographic location and data quality; thus, they must be determined for each data set. We used the MATLAB function "stepwiselm" on the first occupation to determine the optimal parameters to use. This function uses a *t* test to determine which parameters are significant. Temperature, salinity, AOU, silicate, TA, nitrate (NO_3^-), and phosphate (PO_4^{3-}) were considered. We use temperature and AOU rather than potential temperature and oxygen for consistency with earlier studies in this area [*Wanninkhof et al.*, 2010]. Phosphate was found to be unnecessary, although it could be used instead of nitrate. The choice of nitrate over phosphate was made for consistency with earlier studies and because phosphate is not always available for older cruises. We used the same isopycnal surfaces proposed by *Gruber* [1998] and used in other eMLR studies [*Lee et al.*, 2003; *Wanninkhof et al.*, 2010], resulting in 23 separate fits for each occupation. Four separate sections, each occupied three times, resulted in 276 individual MLR fits. Isopycnals were calculated using absolute salinity and TEOS-10 MATLAB equations [*McDougall and Barker*, 2011]. The coefficients for the eMLRs and error statistics are given in the supporting information. An additional isopycnal range of $\sigma_4 > 45.963$ was added for A16 GOSHIP and CLIVAR occupations in order to cover the full water column in the far South Atlantic. The optimal parameters vary by density surface, with deep isopycnals often requiring fewer parameters because of lower spatial variability. The final choice was determined by the fewest number of parameters required to fit all density surfaces so that all fits used the same parameters.

For A16, when S, T, AOU, NO_3^-, and Si are used, as was done in *Wanninkhof et al.* [2010], there is an anomalous penetration of ΔC_{anthro} into the deep North and South Atlantic, far deeper than expected. Such a deep penetration is not supported by transient tracers such as CFCs and SF_6. Use of total alkalinity in place of Si does not show this penetration. This anomaly is attributed to frontal movement and sharp, nearly vertical Si gradients in the intermediate waters of the South Atlantic. A detailed analysis of such potential biases (Appendix A) is important when using an eMLR. Comparisons of the A16 CLIVAR-SAVE eMLR using Si or TA is difficult because of the limited data to fit and because there is more scatter as a result of lower quality

(calculated) TA data for the A16 SAVE cruise, adding significant uncertainty particularly for the southern section. Since a good fit cannot be made using TA data for the A16 SAVE cruise, Si was used for the A16 GOSHIP-SAVE eMLR. Using different independent variables for the eMLR for the different time periods leads to reasonable qualitative results, but the errors are larger (8–10 μmol kg^{-1}, Table S1 in the supporting information), particularly for the intermediate waters (~1500–3000 m) of the South Atlantic. For this reason only the qualitative results for this period are discussed. For the other sections there is no significant difference in the results whether using Si or TA, except for a couple of small areas in A22 and A10. On A22, an area at the bottom around 29–31°N shows an unexpected ~5 μmol kg^{-1} ΔC_{anthro} when using Si in the eMLR (not shown), while in the TA eMLR it is near zero, as expected. For this reason and for consistency, TA is used instead of Si.

The root-mean-square standard error (RMSE) in our MLR fits ranges from 1.2 to 9.9 μmol kg^{-1} (see supporting information), with higher errors near the ocean surface as a result of higher seasonal dynamics in the parameters, and small increases in the very deep waters as a result of limited data, and small ranges in the independent parameters. The densest waters on the SAVE cruise ($\sigma_4 > 45.963$) had errors over 10 μmol kg^{-1} due to the low resolution of the measurements and were excluded from further analysis (see section 2). After each MLR was fit, the residuals were inspected for outliers and biases. No biases were found.

Accurate determination of the uncertainty of this method is challenging. One of the major advantages of the eMLR results from using the differences in the coefficients which largely cancel out random variability and error in the independent parameters [*Friis et al.*, 2005; *Wanninkhof et al.*, 2010]. A detailed discussion found in *Waters et al.* [2011] identifies the assumptions inherent in the MLR fits as the largest source of uncertainty in this method. The average RMSE of all MLRs is 2.6 μmol kg^{-1} (see supporting information). We use this value as the error resulting from the fit. *Friis et al.* [2005] determined the error from uncertainties in the independent parameters to be 1 μmol kg^{-1}. Combining this with the error in the fit gives 2.8 μmol kg^{-1}. We round this to 3 μmol kg^{-1} to be conservative. This agrees with previous studies [*Lee et al.*, 2003; *Sabine et al.*, 2004; *Friis et al.*, 2005; *Murata et al.*, 2008; *Wanninkhof et al.*, 2010; *Waters et al.*, 2011] and is also supported by deep values which are not expected to have any ΔC_{anthro}, showing ΔC_{anthro} of less than 3 μmol kg^{-1}.

4.2. Treatment of Surface Data

The surface is the most difficult to fit due to large natural (seasonal) variability. Previous studies dealt with the increased surface variability in a variety of ways, such as excluding the surface from the eMLR and then extrapolating from the bottom of the mixed layer [*Brown et al.*, 2010], assuming that the pCO_2 in the surface changes at the same rate as the pCO_2 in the atmosphere [*Sabine et al.*, 2008; *Waters et al.*, 2011] or applying the eMLR all the way to surface [*Friis et al.*, 2005; *Wanninkhof et al.*, 2010].

When cruises were conducted in different seasons, we used the methods employed by *Sabine et al.* [2008] and *Waters et al.* [2011] for the surface. It assumes that the rate of change for fugacity of CO_2 (fCO_2) in the top 150 m is the same as the value in the atmosphere. This was verified by checking the change in surface fCO_2, which was 17.2 ± 60.0 μatm (unless stated otherwise, all values are mean ± standard deviation), very close to the 19.9 ppm increase in the atmosphere over that time period. The increase in atmospheric CO_2 (i.e., 20 ppm for 2003–2012) is converted into an equivalent change in TCO_2 using CO2sys and assuming constant TA. This method is weakly dependent on the assumption that TA does not change significantly between the cruises.

For cruises in the same season, *Wanninkhof et al.* [2010] argue that the eMLR can be extended all the way to the surface, thus eliminating the need for extra assumptions. This only holds if there is no significant interannual variability, which was checked by correspondence in T and S between the occupations. This could only be done for A16. For the A16 GOSHIP-CLIVAR occupations we compare both methods. The average difference in ΔC_{anthro} between the two methods (eMLR − constant ΔfCO_2) is 3.92 ± 3.98 μmol kg^{-1}, which is only slightly higher than the uncertainty. There are, however, clear regional biases. The differences are largest in polar and equatorial regions and approach zero or become negative in the subtropical/tropical regions. This indicates that at least in this case the eMLR method will produce slightly higher estimated changes at the surface than other methods and that the biases will vary regionally. The difference is small for the total inventory change (0.2 Pg C decade^{-1} in the North Atlantic). Although there is ample evidence that the average surface ocean fCO_2 is increasing at nearly the same rate as the atmosphere, including the observations of surface water CO_2 levels on these cruises, there is still large variability regionally as well as seasonally

[*Hood et al*., 1999; *Jones et al*., 2014] and between El Niño and non–El Niño years [*Feely et al*., 2006] that are not captured in the constant ΔfCO_2 method. The eMLR method does not require these additional assumptions. When the eMLR is applied along density surfaces, then the surface cannot influence deeper waters, which is confirmed by comparison of the two methods below the mixed layer. No differences are observed, demonstrating that surface variability does not contaminate deeper waters.

4.3. Determining Anthropogenic pH Changes

Uptake of anthropogenic CO_2 also decreases the pH. Determining the change in pH is more challenging than determining ΔC_{anthro} since pH is highly temperature dependent and therefore shows higher natural variability. Also, direct high-quality measurements of pH only became common practice during the CLIVAR era, and although highly precise, there is uncertainty in the accuracy [*Yao et al*., 2007]. Currently, no standard or certified reference material is available, making it difficult to compare cruises from different times and to separate natural variability from anthropogenic decreases. Further compounding the difficulties is that different groups measure pH at different temperatures (typically either 20°C or 25°C), and the conversion into the in situ temperature and pressure requires either another carbon parameter, or an empirical relationship [*Millero*, 1995], which further increases the uncertainty in the results. Moreover, the pressure dependency of pH is not well constrained (K. Johnson, MBARI, personal communication, 2015).

The eMLR techniques have been used to calculate the anthropogenic change in pH (ΔpH_{anthro}) [*Andreev et al*., 2009]. Although the variations in pH are directly related to changes in TCO_2, variability in pH is nonlinear which can invalidate assumptions of the eMLR. An eMLR was done for A16 GOSHIP-CLIVAR, and although the results were reasonable qualitatively, the errors were similar to, or larger than, expected anthropogenic changes indicating that the eMLR is not appropriate for determining ΔpH_{anthro}. Instead, we calculate the ΔpH_{anthro} from the ΔC_{anthro} and the assumption that total alkalinity does not change significantly. This is very similar to the technique of *Byrne et al*. [2010] except that they used the ΔC^* method to calculate ΔC_{anthro} and pH at 25°C, while we use in situ pH. The pH on the seawater scale was calculated from TCO_2 and TA (along with silicate and phosphate) at in situ temperature and pressure using the carbonate constants of *Millero et al*. [2006], the HSO_4^- constant of *Dickson* [1990], borate constant of *Uppstrom* [1974], and the pressure dependency of *Millero* [1995]. All calculations were made using the MATLAB CO2sys version 1.02 [*van Heuven et al*., 2009]. The ΔC_{anthro} is then subtracted from the measured TCO_2, and the pH is recalculated to provide an estimate of what the pH would be without any anthropogenic influence (pH_{NAT}). The difference between the two pH values equals the ΔpH_{anthro}. Determining the error in this calculation is difficult, but assuming an error in ΔC_{anthro} of ~3 $\mu mol\ kg^{-1}$ results in an error in ΔpH_{anthro} of ~0.005. This uncertainty would be higher if TA does not remain constant, which is the case for some areas in these data sets. A greater precision can be obtained using discrete pCO_2 along with TA or TCO_2. [*Patsavas et al*., 2015; *Wanninkhof et al*., 2013] to determine the pH change. However, discrete pCO_2 was not measured on all the cruises or only measured at low spatial resolution.

5. Anthropogenic CO_2 Increases

The ΔC_{anthro} for all cruises (Figures 3 and 4) show similar general patterns. There is high ΔC_{anthro} in subtropical surface waters, and deeper penetration at high latitude where deep and intermediate water formation occurs. For A16 (Figures 3a and 4a), ΔC_{anthro} is detectable all the way to the bottom (~3000 m) in parts of the North Atlantic as a result of NADW formation. There is also a significant amount of ΔC_{anthro} in Antarctic Intermediate Water down to ~2000 m in the South Atlantic. We also determined the ΔC_{anthro} for the CLIVAR-SAVE period for comparison with *Wanninkhof et al*. [2010] and as a check on our calculations (given in the supporting information). The two were in good agreement; our results show slightly, but not significantly, lower values in the North Atlantic.

To the west of the A16 line, A20 (Figures 3b and 4b) extends from Nova Scotia, Canada, down to the coast of South America, north of French Guiana. Unlike the A16 section, this transect only encompasses 15 years, but the results are similar. The largest change of ΔC_{anthro} with depth is in the northern portion with a shoaling toward the south, as is also seen in A16 over the same latitude range. The deeper penetration in the north is associated with Labrador Sea Water [*Macdonald et al*., 2003; *Tanhua et al*., 2006]. For the most recent 10 years, there is no ΔC_{anthro} below 1000 m, the maximum is around 700 m in the northern portion and only around 300 m closest to South America. This is likely a result of older Antarctic Intermediate Water (AAIW)

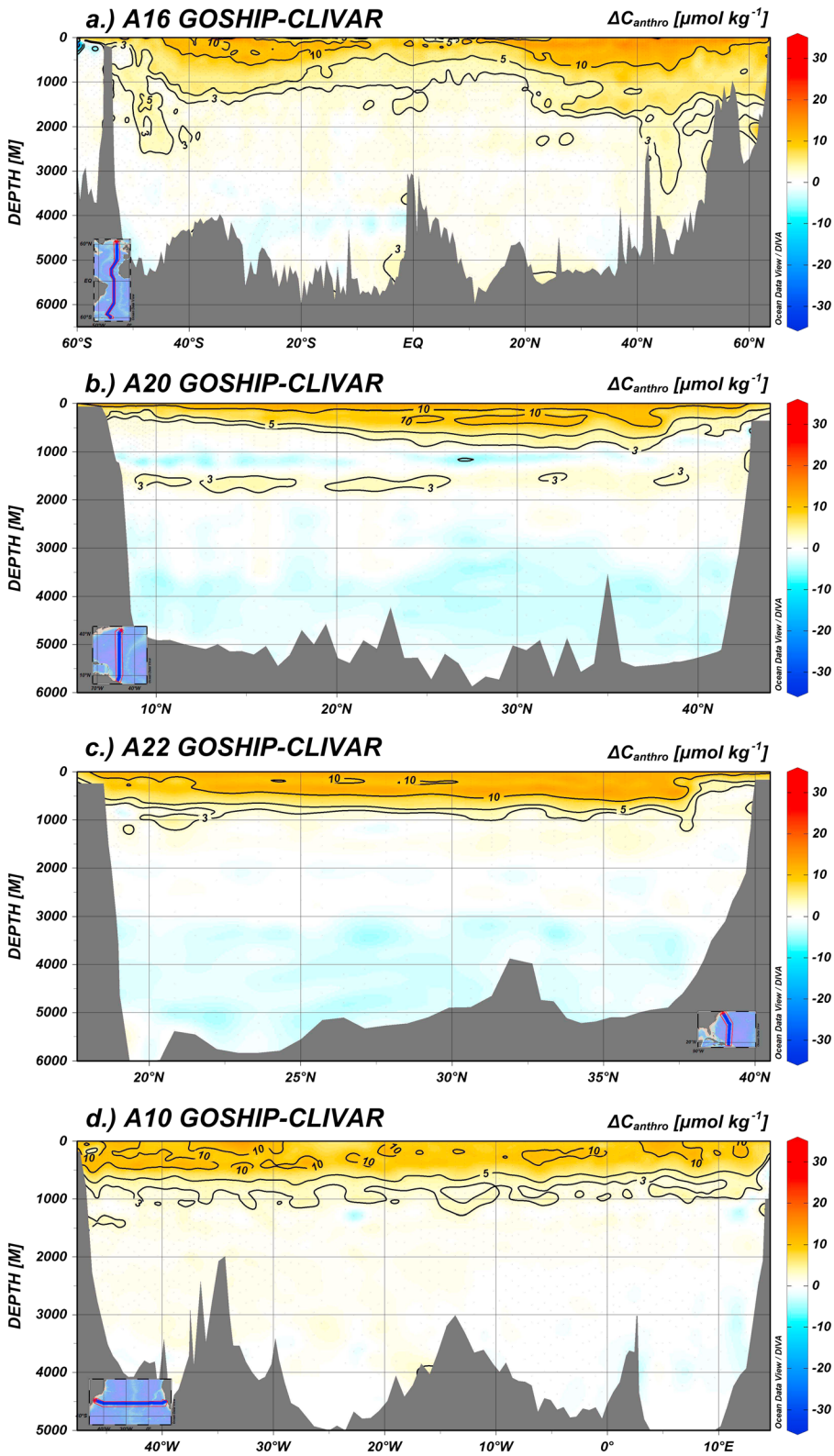

Figure 3. ΔC_{anthro} along the four sections for the GOSHIP to CLIVAR time periods. (a) A16, (b) A20, (c) A22, and (d) A10.

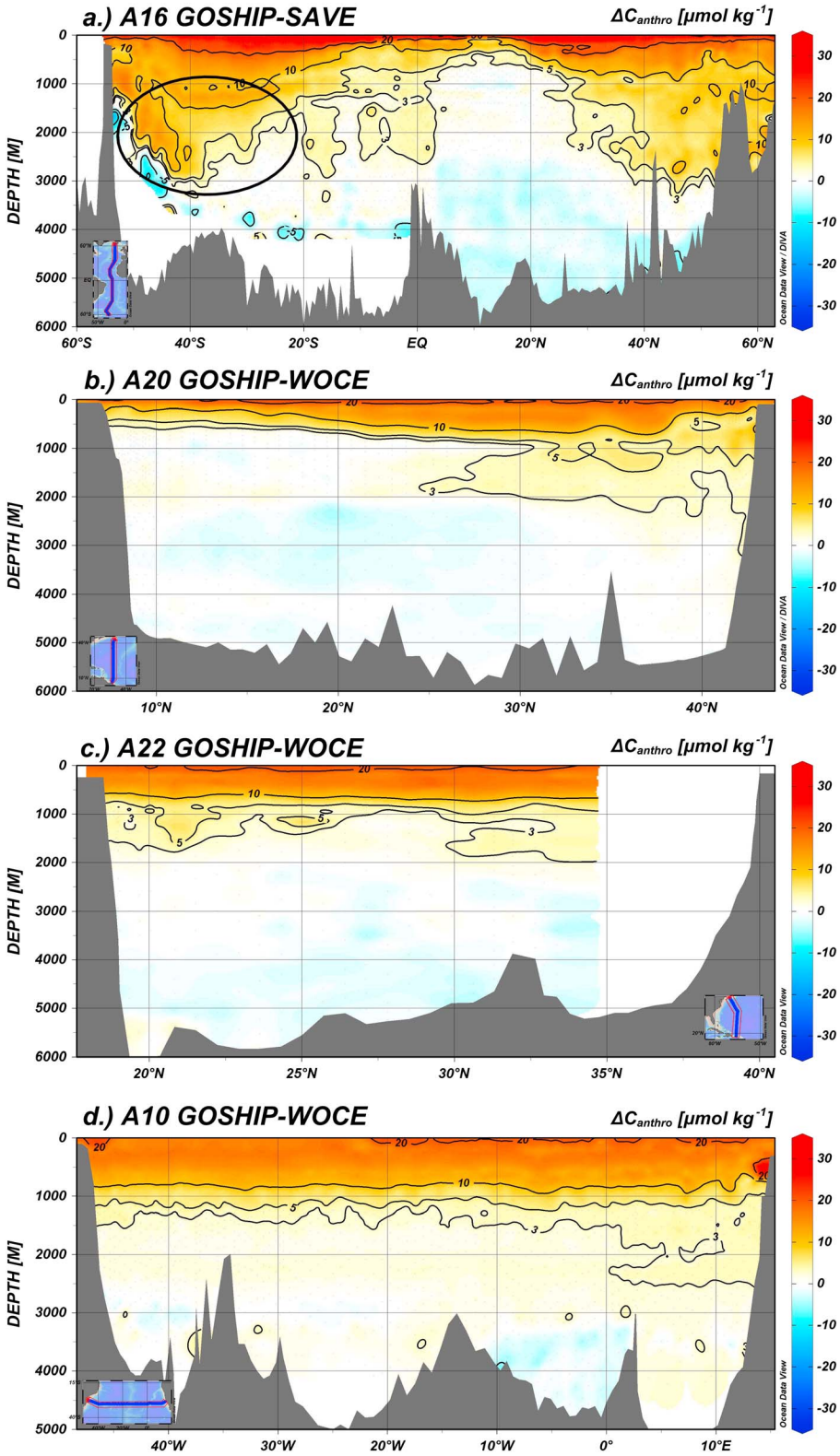

Figure 4. ΔC_{anthro} along the four sections for the time GOSHIP to WOCE/OACES/SAVE time periods in (a) A16, (b) A20, (c) A22, and (d) A10. The area circled in black in the South Atlantic in Figure 4a is thought to be overestimated as a result of using Si in the eMLR.

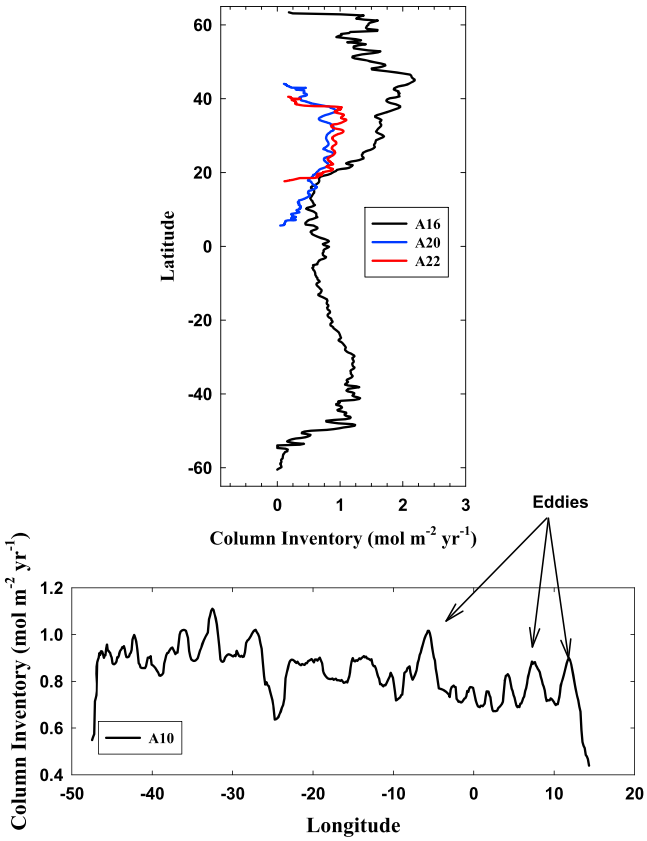

Figure 5. Specific column inventories for all four cruises as an annual rate calculated over the GOSHIP-CLIVAR time periods (2003–2005 to 2011–2014). Inventories were determined by integrating from the surface to the depth of significant ΔC_{anthro} (3 μmol kg^{-1}).

and Upper Circumpolar Deep Water (UCDW) located around 800 m [*Macdonald et al.*, 2003; *Brown et al.*, 2010]. The 3 μmol kg^{-1} contour found at around 1400 m is likely the Upper Labrador seawater component of the NADW cutting diagonally across the section; this is supported by a peak in CFC concentrations at the same depth. Over the 15 year period, there is ΔC_{anthro} down to around 1500 m in the North and about 500 m in the south.

A22 (Figures 3c and 4c) is about 12° farther west and is very similar to A20, except that it terminates farther north near the coast of Puerto Rico and there is no shoaling of ΔC_{anthro} in the southern portion of the section. The depth to which ΔC_{anthro} reaches is similar to that found on A20. Over the GOSHIP-CLIVAR period, ΔC_{anthro} reaches down to about 700 m, except in the northernmost portion near New England. Shoaling of ΔC_{anthro} in this section is very sharp and marks the boundary of the Deep Western Boundary Current [*Joyce et al.*, 2001]. Unlike A16 and A10, no studies have looked at the anthropogenic carbon storage between the CLIVAR and WOCE A20 and A22 cruises so there are no direct comparisons that can be made for these meridional cruises. *Brown et al.* [2010] used the eMLR method for a zonal transect from Florida to Africa along 24.5°N and found ΔC_{anthro} changes down to a maximum of ~800 m in the western Atlantic Basin for the period 1992–2004, similar to our results. *Macdonald et al.* [2003] looked as the same region as *Brown et al.* [2010] but considered the entire Industrial era, so we can only compare qualitatively to their results. They found high C_{anthro} in the surface, with a sharp gradient around ~800 m associated with UCDW/AAIW, which is very similar to the pattern found in our results.

The only zonal transect used in this study is along the A10 section in the South Atlantic (Figures 3d and 4d). There is a small east/west difference with a near constant change to a depth of about 750 m from the GOSHIP-CLIVAR period and to about 1200 m for the CLIVAR-WOCE period. There is a slight shoaling of less than 100 m in the area east of the prime meridian. The isopycnals are fairly flat in the east-west direction implying that intermediate waters are not ventilated at this latitude, and therefore, there is no penetration pathway of CO_2 along this transect; instead, ΔC_{anthro} is largely transported north/south across the section. These results are similar to *Murata et al.* [2008], who looked at the CLIVAR-WOCE period, using a ΔC^* method, correcting for remineralization changes. They also found less penetration in the eastern than in the western basin.

There is only one crossover point in the four sections. It is between A16 and A10 located at 25°W, 30°S. For the deep waters, the difference between A16 and A10 ΔC_{anthro} is 1.6 ± 1.7 μmol kg^{-1}. For comparison of ΔC_{anthro} between the different cruise periods, the values are converted into a rate. For the GOSHIP-CLIVAR era at the cross-over location the rates were very similar 1.04 ± 0.28 and 0.98 ± 0.17 μmol kg^{-1} yr^{-1} for A16 and A10, respectively. For the GOSHIP-WOCE/GOSHIP-SAVE era crossover, the rates were 0.73 ± 0.31 and 0.75 ± 0.23 μmol kg^{-1} yr^{-1} for

A16 and A10, respectively. The A16 GOSHIP-SAVE likely overestimates ΔC_{anthro} in the intermediate depths between ~1000 and 2500 m, as a result of using Si instead of TA in the eMLR. All the rates are in general agreement with previous studies in the region [*Murata et al*., 2008; *Wanninkhof et al*., 2010].

6. Estimating ΔC_{anthro} Inventory Change in the Atlantic

A main goal is to estimate the total decadal accumulation of ΔC_{anthro} for the entire Atlantic basin. The overall rate of atmospheric CO_2 change has been increasing significantly over the last few decades. From 1995 to 2005, atmospheric CO_2 increased at a rate of 1.87 ppm yr^{-1}, and from 2005 to 2014 at a rate of 2.11 ppm yr^{-1} [*Canadell et al*., 2007]. As a result, a proportional increase in the oceanic uptake is expected. Estimating decadal inventory changes of ΔC_{anthro} is challenging due to large uncertainties caused by limited spatial and temporal coverage, natural variability, and methodological issues, as described above. The column inventories were estimated for each section by integrating the gridded data from the surface down to 3 μmol kg^{-1} contour line. These values are then normalized to an annual basis for direct comparisons (Figure 5). The overall pattern for A16 agrees well with that found by *Wanninkhof et al*. [2010]; however, our values are higher. For the South Atlantic, the results for the last 10 years are similar to the previous 10 years [*Wanninkhof et al*., 2010]. Our values are slightly larger, but within the uncertainty, and a larger value is expected due to the increased rate of atmospheric CO_2 rise due to anthropogenic emissions [*Canadell et al*., 2007]. The North Atlantic shows significant increases, as much as double for the previous decade compared to *Wanninkhof et al.*'s [2010] Table A1. There are no previous studies published on ΔC_{anthro} for A20 and A22. The study of the CLIVAR-WOCE A10 of *Murata et al*. [2008] estimate an average uptake rate of 0.6 ± 0.1 mol m^{-2} yr^{-1} for the entire section between 1992/1993 and 2003, which is in reasonable agreement with our average of 0.83 ± 0.1 mol m^{-2} yr^{-1}. Based on Table 3 in *Murata et al*. [2008], for the eastern and western basin, rates are 0.81 mol m^{-2} yr^{-1} and 0.46 mol m^{-2} yr^{-1}, respectively. These values compare to our average values of the eastern and western basin of 0.88 ± 0.04 mol m^{-2} yr^{-1} and 0.78 ± 0.1 mol m^{-2} yr^{-1}, respectively. The eastern basin is in good agreement between the two studies. The differences in the western basin are discussed below.

A10 shows a decrease in column inventory west to east, which is masked by peaks centered around 5°W, 8°E, and 11°E. These peaks are the result of eddies as indicated by changes in T, S, Si, TCO_2, and other properties between the two occupations (not shown). The column inventories inside the eddies average 0.12 mol m^{-2} yr^{-1} higher than the inventories in the immediately surrounding areas. That results in approximately 20% more anthropogenic carbon than the immediately surrounding waters. This highlights the importance of eddies in transporting ΔC_{anthro} laterally and that they play a significant role. It is important to note, however, that it is uncertain how well the eMLR is able to resolve eddies. Most studies of mesoscale processes and eddies in transporting anthropogenic carbon are limited to Global Circulation Models [*Lachkar et al*., 2009; *Ito et al*., 2010; *Gnanadesikan et al*., 2015], which indicate that eddies do play an important role in transporting C_{anthro} with values similar to the 20% found here. We are not aware of any other studies that directly observe C_{anthro} transported by eddies. Although *Ríos et al*. [2003] identified eddies transporting anthropogenic carbon, this is the first study we are aware of to fully quantify this transport with direct measurements. More studies into the influence of eddies on transporting ΔC_{anthro} are warranted.

A big methodological challenge is how to extrapolate from a few sections to the entire basin. A16 is often considered to be representative of the entire Atlantic since it transects the entire basin [*Wanninkhof et al*., 2010]; however, there are considerable east/west trends [*Gruber et al*., 1996; *Brown et al*., 2010] as seen in Figure 5. The inventory can vary by greater than 50% for a given latitude, making it difficult to extrapolate over the entire basin. We use two different methods of extrapolating over the entire basin for the GOSHIP-CLIVAR era (2000s). Both rely on averaging the column inventory over longitudinal bands and multiplying by volume of water in that band. The volumes were taken from *Gruber* [1998]. The first method uses only A16 to represent the entire basin, this makes for a direct comparison with *Wanninkhof et al*. [2010]. The second method divides the Atlantic into east and west sections. For the North Atlantic, A20 and A22 were used to represent the western basin and A16 the eastern basin. For the South Atlantic, A16 was used for latitudinal distribution and A10 was used to determine longitudinal distribution. The results, along with values from several other studies, are given in Table 2. Following the analysis of *Lee et al*. [2003] and *Wanninkhof et al*. [2010], we estimate an error of 20% or $\pm$ 1.6 Pg C $decade^{-1}$ for the entire Atlantic. The total anthropogenic uptake for the North and South Atlantic is 8.1 Pg C $decade^{-1}$, compared to the total (natural plus anthropogenic) change

Table 2. Comparison of Different Inventories of Anthropogenic Carbon for the Entire Atlantic Basin in Pg C decade^{-1}[a]

	2000s		1990s		
Latitudinal band	A16 only	Weighted[b]	Wanninkhof[c]	BEC model[d]	Mikaloff[e]
60–50°S	0.12	0.12	0.49		
50–40°S	0.84	0.89	0.68		
40–30°S	1.04	0.97	0.80		
30–20°S	0.89	0.75	0.68		
20–10°S	0.60	0.51	0.37		
10°S to the equator	0.47	0.45	0.20		
Southern Hemisphere	4.0	3.7	3.2	3.4	3
Equator to 10°N	0.54	0.50	0.21		
10–20°N	0.55	0.51	−0.11		
20–30°N	1.19	1.10	0.48		
30–40°N	1.38	0.96	0.54		
40–50°N	1.24	0.61	0.41		
50–60°N	0.78	0.75	0.39		
Northern Hemisphere	5.7	4.4	1.9	1.1	2.9
Total	9.7	8.1	5.1	4.5	5.9

[a]The inventories in this study were calculated using two different methods. The first, extrapolating A16 over the entire basin and the second, extrapolating using all four sections.
[b]Uses all four sections to account for longitudinal variation. Details in text.
[c]*Wanninkhof et al.* [2010] covering the period 1989–2005.
[d]*Doney et al.* [2009].
[e]*Mikaloff Fletcher et al.* [2006]. Centered on 1995.

in TCO_2 of 10.6 Pg C decade^{-1}. This means that three quarters of the total changes in TCO_2 can be attributed to anthropogenic uptake and storage.

There is excellent agreement between all six estimates for the South Atlantic. For the North Atlantic there is much more spread in the values between time periods. We found an increase in the ΔC_{anthro} of the North Atlantic for the GOSHIP-CLIVAR period compared to the CLIVAR-WOCE period; thus, our estimates of total carbon storage are larger than previous studies. Comparing the A16 inventory with *Wanninkhof et al.* [2010] shows more than twice the CO_2 uptake by the North Atlantic over the last decade. Some of this difference could be a result of the slight difference in eMLR parameters (see Appendix A), but the difference is much larger than the uncertainty. Even taking longitudinal differences into account, we calculate a total carbon inventory change twice the value of *Wanninkhof et al.* [2010], which is larger than our estimated uncertainty. Of the other studies, our value is in closest agreement with *Mikaloff Fletcher et al.* [2006] but still indicates an increase in the uptake of carbon in the North Atlantic over the last decade. Large variability in the uptake rate on subdecadal scales in the North Atlantic has been documented by others [*Pérez et al.*, 2010, 2013; *Steinfeldt et al.*, 2009]. A high North Atlantic Oscillation (NAO) index corresponds to periods of high carbon storage [*Pérez et al.*, 2010; *Brown et al.*, 2010]. Our rates are in good agreement with *Pérez et al.* [2010, 2013] for high NAO periods. From 1989 to 1995 the NAO was in a high positive phase, followed by a negative phase starting in 2002 [*Pérez et al.*, 2013], after a minimum in 2010 the NAO has been rapidly increasing (see https://climatedataguide.ucar.edu/climate-data/hurrell-north-atlantic-oscillation-nao-index-pc-based). Recent studies showing large annual and decadal variation in the strength of the Atlantic

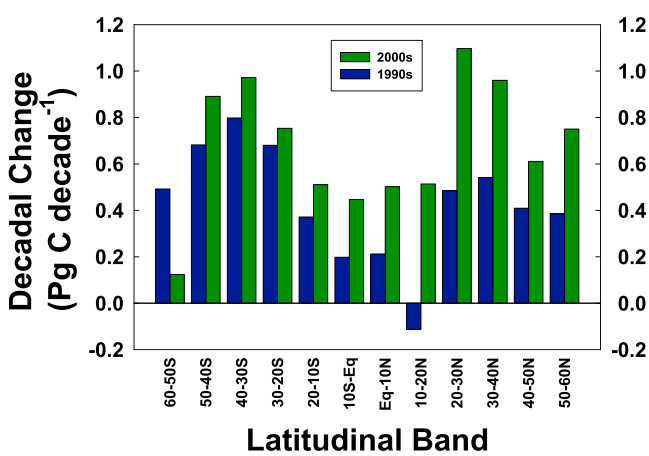

Figure 6. Decadal inventories in Pg C decade^{-1} for the 1990s and 2000s. The 1990 data are from *Wanninkhof et al.* [2010]; 2000s data are the basin weighted values.

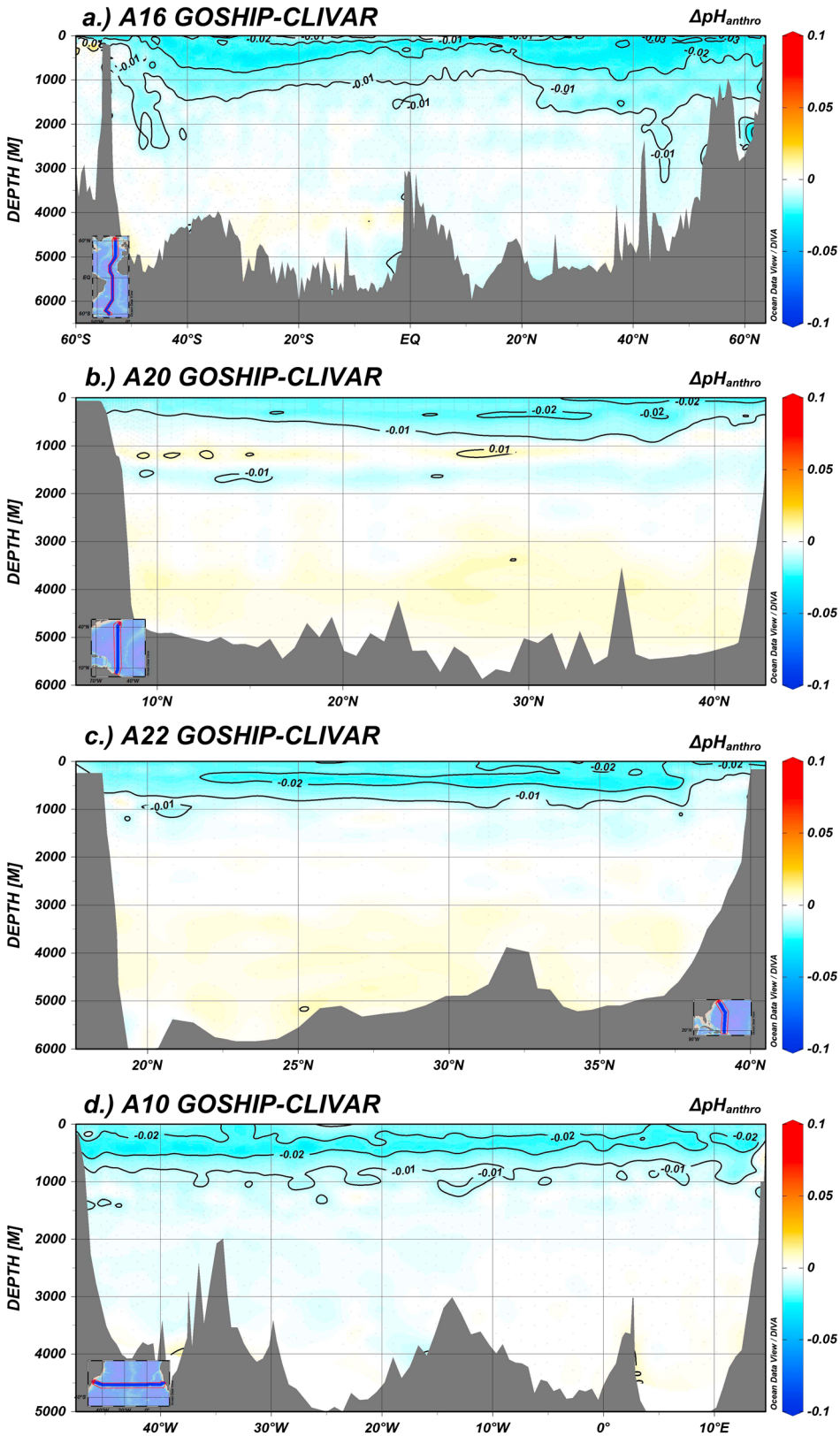

Figure 7. ΔpH_{anthro} along the four sections for the GOSHIP-CLIVAR era for (a) A16, (b) A20, (c) A22, and (d) A10.

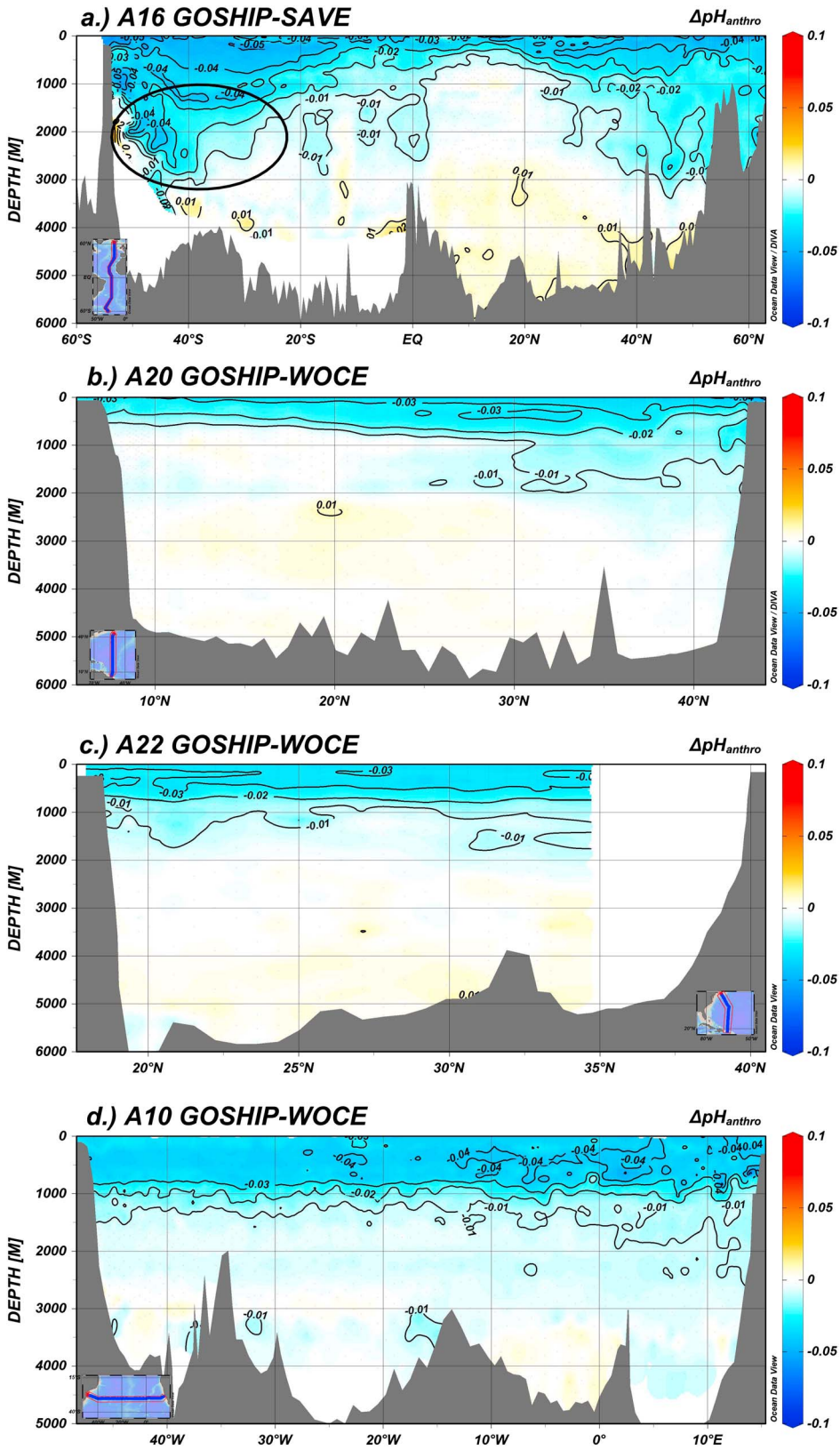

Figure 8. ΔpH_{anthro} along the four sections for GOSHIP-WOCE/OACES/SAVE era for (a) A16, (b) A20, (c) A22, and (d) A10. The area circled in black in the South Atlantic in Figure 8a is thought to be overestimated as a result of using Si in the eMLR.

Table 3. Rates of Ocean Acidification in the Upper 250 m Expressed as Decrease in pH in pH Units per Year for the Four Different Sections for the GOSHIP-CLIVAR Era, the CLIVAR-WOCE/CLIVAR-SAVE Era, and the Overall GOSHIP-WOCE/GOSHIP-SAVE Periods

	GOSHIP-CLIVAR		CLIVAR-WOCE/CLIVAR-SAVE		GOSHIP-WOCE/GOSHIP-SAVE	
Section	Rate	Standard Deviation	Rate	Standard Deviation	Rate	Standard Deviation
A10	−0.0022	0.0004	−0.0020	0.0003	−0.0020	0.0003
A16	−0.0021	0.0010	−0.0011	0.0005	−0.0016	0.0004
A20	−0.0020	0.0004	−0.0019	0.0005	−0.0021	0.0003
A22	−0.0021	0.0003	0.0020	0.0007	−0.0021	0.0003
All	−0.0021	0.0007	−0.0013	0.0008	−0.0018	0.0004

meridional overturning circulation which can vary by 30% annually [*Srokosz and Bryden*, 2015] could also contribute to decadal variations in carbon uptake, particularly in the tropical North Atlantic [*Pérez et al.*, 2013; *Zunino et al.*, 2015].

A comparison of our decadal inventories for the 2000s with those for the 1990s from *Wanninkhof et al.* [2010] (Figure 6) shows the distribution of the increased inventory observed over the last 10 years. The general pattern is the same for both decades, but the areas of increased storage become readily apparent. The North Atlantic shows an overall increase at all latitudes. This indicates that the increases observed are a result of transport to the interior ocean through NADW formation. The South Atlantic shows very similar inventories over the two time periods, although our values tend to be slightly larger.

7. Anthropogenic pH Decreases

The decreases in pH as a result of CO_2 uptake are important for their potential impacts on calcifying and other organisms. The decreases in pH as a result of this uptake of anthropogenic CO_2 follow the same distribution pattern as $\Delta C_{anthro,}$ as expected since it is calculated from ΔC_{anthro} (Figures 7 and 8). As seen in A16, the maximum decreases are in the polar regions. None of the previous studies which used the eMLR technique also looked at changes in pH, so direct comparisons are not possible. For A20 and A22, the patterns match that of ΔC_{anthro} with pH decreasing significantly and fairly uniformly to about 750 m from GOSHIP-CLIVAR and to around 1000 m from GOSHIP-WOCE. For A10, there is a significant decrease in pH down to about 750 m for the GOSHIP-CLIVAR period and down to about 1200 m for the GOSHIP-WOCE period. There is a subsurface minimum centered around 400 m which is attributed to sub-Antarctic Mode Water.

For the crossover point for A16 and A10 the deep waters are in good agreement for all four profiles. Differences are within 0.005 pH units, within the uncertainty estimates. The rates of change in pH for the GOSHIP-CLIVAR era cruises are $-0.0022 \pm 0.0007\ yr^{-1}$ and $-0.0023 \pm 0.0004\ yr^{-1}$ for A16 and A10, respectively; and for the GOSHIP-WOCE era cruises the rates are $-0.0016 \pm 0.0004\ yr^{-1}$ and $-0.0019 \pm 0.0004\ yr^{-1}$ for A16 and A10, respectively. As with ΔC_{anthro}, they are all in good agreement; but the GOSHIP-WOCE era cruises show lower rates than the GOSHIP-CLIVAR era. All of these are close to the expected rate of decrease based on thermodynamics and increasing atmospheric CO_2 levels.

The ocean acidification rate for the surface (upper 250 m) oceans, in pH units per year, was determined for the WOCE to CLIVAR, the CLIVAR to GOSHIP, and the full WOCE to GOSHIP time spans for each section and for the entire basin (Table 3). The overall rate for the GOSHIP-CLIVAR era was $-0.0021 \pm 0.0007\ yr^{-1}$, -0.0013 ± 0.0008 for the CLIVAR-WOCE/CLIVAR-SAVE era, and $-0.0018 \pm 0.0004\ yr^{-1}$ for the entire GOSHIP-WOCE/GOSHIP-SAVE era. These are in agreement with other studies in the Pacific and Atlantic which range from -0.0014 to $-0.0022\ yr^{-1}$ [*Bates*, 2007; *González-Dávila et al.*, 2007; *Byrne et al.*, 2010; *Waters et al.*, 2011; *McGrath et al.*, 2012; *Vázquez-Rodríguez et al.*, 2012; *Lauvset and Gruber*, 2014; *Ríos et al.*, 2015; *Williams et al.*, 2015]. This is also in agreement with the value $-0.0018\ yr^{-1}$ expected based on thermodynamics and the rate of increase of CO_2 in the atmosphere [*Waters et al.*, 2011]. The low value for the A16 CLIVAR-WOCE/CLIVAR-SAVE period is interesting because it is slightly lower than expected from CO_2 exchange with the atmosphere, and lower than other studies. The increase to a more typical value during the GOSHIP-CLIVAR period demonstrates that the 1990s was a period of low CO_2 uptake for the North Atlantic.

8. Conclusions

From 1989 to 2014 the Atlantic Ocean has experienced significant changes in uptake and storage of anthropogenic carbon. The largest changes in column inventories are located in the polar regions, with the North Atlantic having the highest column inventory as a result of deep water formation. The total basin-wide accumulation shows significant decadal variability, with much higher accumulation in the 2000s than in the 1990s. This variability appears to be largely related to the NAO. The entire Atlantic absorbed 8.1 ± 1.6 Pg C in the 2000s compared to 5 ± 1 Pg C in the 1990s. The accumulating CO_2 results in a decrease in pH at an overall rate of $-0.0021 \pm 0.0007\ yr^{-1}$ in the surface ocean, similar to the predicted rate based on the rate of CO_2 increase in the atmosphere. Eddies were observed to contain significant amounts of anthropogenic carbon in the South Atlantic. The decadal variability in the storage of anthropogenic carbon, particularly for the North Atlantic, highlight the importance of future repeat hydrography cruises in understanding and quantifying decadal variability in the uptake of anthropogenic carbon by the oceans.

9. Data Availability

All data used in this analysis can be found at CDIAC (http://cdiac.ornl.gov/oceans/bottle_discrete.html) and CCHDO (http://cchdo.ucsd.edu/search?bbox=-75,-60,20,65).

Appendix A: Important eMLR Considerations

The eMLR has advantages compared to other methods to determine ΔC_{anthro} as noted in the text, but there are some caveats. The MLR approach, from a statistical standpoint, should be applied to independent data that are not cross correlated to avoid overfitting [*Thacker*, 2012]. Most parameters used in the MLR to determine ΔC_{anthro} do have strong inherent dependencies. Several other criteria for use of the MLR technique are not fulfilled in oceanographic applications. Moreover, the choice of independent parameters to reflect the natural variability in TCO_2 is subjective, and results are dependent on the choices [see, e.g., *Plancherel et al*., 2013]. This is important to consider when selecting the independent parameters and when interpreting the results. When dealing with older data sets the choices are often limited by data quality and availability, but with more recent data sets which have high quality and high resolution there is more flexibility. The results from the A16 GOSHIP-CLIVAR eMLR highlight the importance of selecting the proper independent variables and some of the limitations of the eMLR method. The result of the eMLR for A16 GOSHIP-CLIVAR using S, T, AOU, NO_3^-, and Si is given in Figure A1a. A comparison to the same figure created using TA instead of Si (Figure 3a) shows appreciable differences. The most notable being the deep penetration of the 5 $\mu mol\ kg^{-1}$ contour line of ΔC_{anthro} in the South Atlantic using Si as an independent variable. The differences between the two eMLR are shown in Figure A1b. The mean and standard deviation of the difference in ΔC_{anthro} is $0.91 \pm 1.98\ \mu mol\ kg^{-1}$ ($N = 4856$), well within the uncertainty; however, there are clear patterns to the biases, with the Si fit generally having higher ΔC_{anthro} than the TA fit. There is higher ΔC_{anthro} near the bottom of the North Atlantic and significant ΔC_{anthro} down to about 3000 m in the intermediate waters of the South Atlantic, which are not present in the TA fit. These deep penetrations are not expected. Although the absolute value of the bias is small, the volume of water is large so that when integrating the column inventory over the entire basin, it will nearly double the total amount of ΔC_{anthro}. This highlights the impact of parameter choice in such extrapolations and the need to use other indicators such as transient tracers to determine the validity of results.

Figure A1c shows the transient tracer SF_6 measured on A16 GOSHIP. The pattern of ΔC_{anthro} is expected to be similar to that of SF_6 for this time period. The pattern matches very closely with the eMLR using TA, but not with that of Si, suggesting that TA better represents the ΔC_{anthro} for this time period. Si is not directly involved in the inorganic carbon system, but it is often used in eMLRs because of the close correlation between Si and TA in deep waters, and high-quality Si data are more readily available than TA data. This is particularly true for older data, especially before the advent of TCO_2 Certified Reference material (CRMs) in 1991 and TA CRMs around 1996. For newer data sets TA is a better choice because it is an inorganic carbon system parameter and because of the large improvements in precision and accuracy since the early 1990s. The cause of the

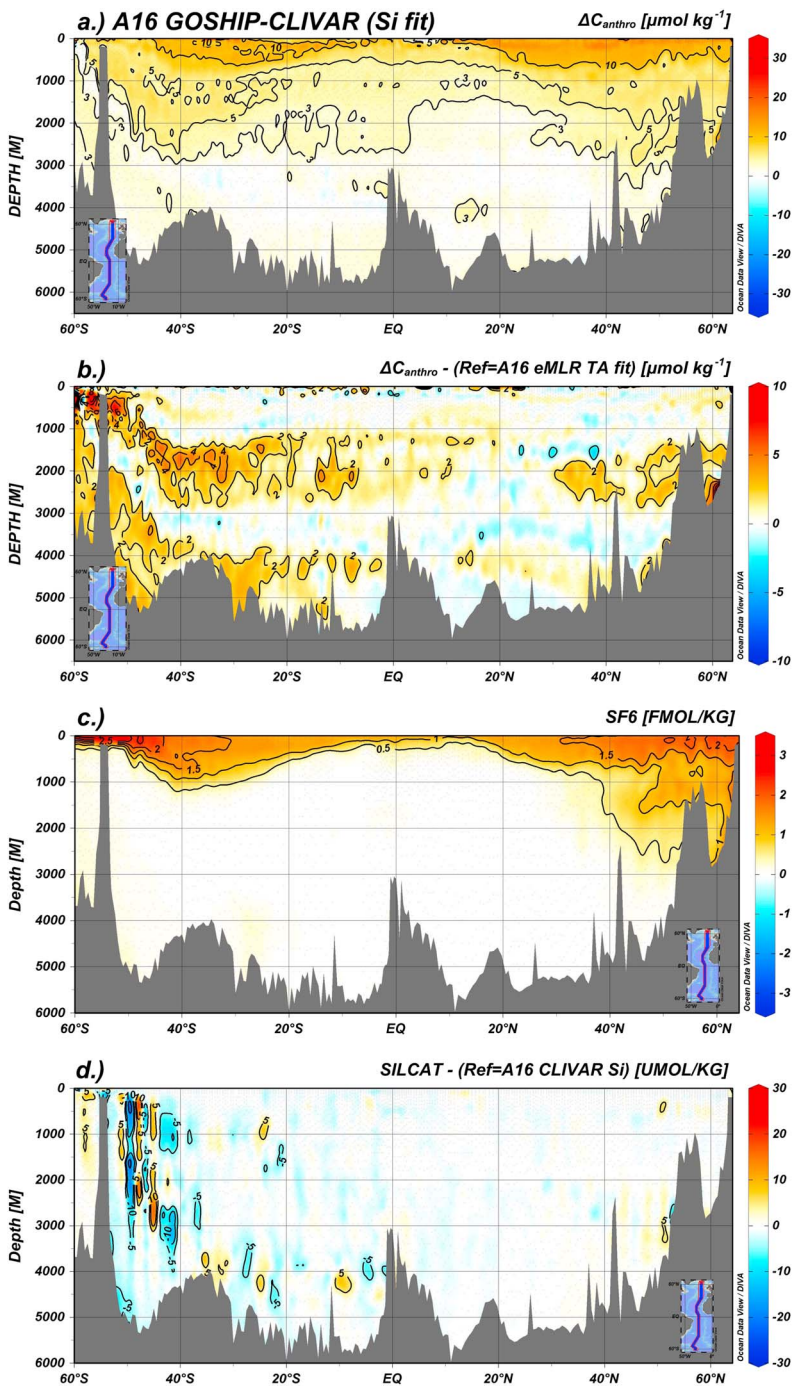

Figure A1. (a) eMLR of A16 GOSHIP-CLIVAR using T, S, AOU, $NO3^{-}$, and Si. There are significant differences when compared to Figure 3a, which uses TA instead of Si. (b) The differences between the two different eMLR fits of the A16 GOSHIP-CLIVAR cruises (eMLR Si fit − eMLR TA fit). There are clear differences in the deep waters of the North Atlantic and intermediate waters of the South Atlantic. (c) Measurement of SF_6 made along A16 GOSHIP (data courtesy of J. Bullister, PMEL). (d) Difference between Si concentrations measured between CLIVAR and GOSHIP occupations of the A16 section (CLIVAR minus GOSHIP).

poor eMLR fit using Si is thought to be related to increases of 5–10 μmol kg^{-1} of Si in the intermediate waters of the South Atlantic, between 2005 and 2014, thought to be caused by movement of fronts (Figure A1d) that are not as readily apparent in the other independent parameters. The eMLR should be able to account for such changes, but Si is not linearly related to TCO_2 along the isopycnals where these changes occur and thus violate the MLR criteria [*Thacker*, 2012]. That is, the changes occur in an area of high gradients and weak stratification that the eMLR cannot properly capture. Including both Si and TA, as well as PO_4^{3-}, in the MLR fits were considered. Using both Si and TA produced an intermediate result of the individual fits (not shown) and still showed higher than expected ΔC_{anthro} in the intermediate South Atlantic waters, inconsistent with SF_6 measurements. Including phosphate in the fit did not change the results as expected since NO_3^- is already included, and NO_3^- and PO_4^{3-} are closely stoichiometrically related, leading to overfitting artifacts.

Similar comparisons were made of different eMLR fits on the other cruises to determine biases. The choice of either Si or TA did not influence the results for the most part, except in a few small areas. On A22 there was a small area of significant ΔC_{anthro} at the bottom when using Si that was not present when using TA. A similar small area on the easternmost portion of A10 had unexpectedly large changes in ΔC_{anthro} when using Si instead of TA. This is thought to be a breakdown in the Si/TA relationship. Based on this, it is recommended to use TA instead of Si whenever possible.

Acknowledgments
The authors wish to acknowledge the long-term support of the Oceanographic Section of the National Science Foundation and the Climate Observation and Monitoring Division of the Climate Program Office of the National Oceanic and Atmospheric Administration for supporting this study and the U.S. repeat hydrography cruises currently under the auspices of U.S. GOSHIP. The dedication of the many scientists, officers, and crew of the research ships who executed the seagoing work were instrumental to success of the cruises and quality data.

References

Alvarado-Alvarez, R., M. C. Gould, and J. L. Stephano (1996), Spawning, in vitro maturation, and changes in oocyte electrophysiology induced serotonin in *Tivela stultorum*, *Biol. Bull.*, *190*, 322–328.

Andreev, A. G., C.-T. A. Chen, and S. Watanabe (2009), Calculation methods and the distribution of anthropogenic variations of pH values in the Pacific subarctic, *Oceanology*, *49*(3), 418–428, doi:10.1134/S000143700903014X.

Barcelos e Ramos, J., H. Biswas, K. G. Schultz, J. LaRoche, and U. Riebesell (2007), Effect of rising atmospheric carbon dioxide on the marine nitrogen fixer *Trichodesmium*, *Global Biogeochem. Cycles*, *21*, GB2028, doi:10.1029/2006GB002898.

Bates, N. R. (2007), Interannual variability of the oceanic CO_2 sink in the subtropical gyre of the North Atlantic Ocean over the last 2 decades, *J. Geophys. Res.*, *112*, C09013, doi:10.1029/2006JC003759.

Brewer, P. G. (1978), Direct observation of oceanic CO_2 increase, *Geophys. Res. Lett.*, *5*, 997–1000.

Brown, P. J., D. C. E. Bakker, U. Schuster, and A. J. Waton (2010), Anthropogenic carbon accumulation in the subtropical North Atlantic, *J. Geophys. Res.*, *115*, C04016, doi:10.1029/2008JC005043.

Byrne, R. H., S. Mecking, R. A. Feely, and X. Liu (2010), Direct observations of basin-wide acidification of the North Pacific Ocean, *Geophys. Res. Lett.*, *37*, L02601, doi:10.1029/2009GL040999.

Campbell, A. L., S. Mangan, R. P. Ellis, and C. Lewis (2014), Ocean acidification increases copper toxicity to the early life history stages of the polychaete *Arenicola marina* in artificial seawater, *Environ. Sci. Technol.*, *48*(16), 9745–9753, doi:10.1021/es502739m.

Canadell, J. G., C. L. Quéré, M. R. Raupach, C. B. Field, E. T. Buitenhuis, P. Ciais, and G. Marland (2007), Contributions to accelerating atmospheric CO_2 growth from economic activity, carbon intensity, and efficiency of natural sinks, *Proc. Natl. Acad. Sci. U.S.A.*, *104*(47), 18,866–18,870, doi:10.2307/25450516.

Castle, R., R. Wanninkhof, S. C. Doney, J. Bullister, L. Johns, R. A. Feely, B. E. Huss, F. J. Millero, and K. Lee (1998), Chemical and hydrographic profiles and underway measurements from the North Atlantic during July and August of 1993, NOAA Data Rep. ERL AOML-32, Atl. Oceanogr. and Meteorol. Lab., NOAA, Miami, Fla.

Chen, G. T., and F. J. Millero (1979), Gradual increase of oceanic CO_2, *Nature*, *277*, 205–206.

Desrosiers, R. R., J. Desilets, and F. Dube (1996), Early developmental events following fertilization in the giant scallop *Placopecten magel-lanicus*, *Can. J. Fish. Aquat. Sci.*, *53*, 1382–1392.

Dickson, A. G. (1990), Standard potential of the reaction: AgCl(s) + 1/2H_2(g) = Ag(s) + HCl(aq), and the standard acidity constant of the ion in synthetic sea water from 273.15 to 318.15 K, *J. Chem. Thermodyn.*, *22*, 113–127.

Doney, S. C., S. Yeager, G. Danabasoglu, W. G. Large, and J. C. McWilliams (2007), Mechanisms governing interannual variability of upper ocean temperature in a global hind cast simulation, *J. Phys. Oceanogr.*, *37*, 1918–1938, doi:10.1175/JPO3089.1.

Doney, S. C., I. Lima, J. K. Moore, K. Lindsay, M. J. Behrenfeld, T. K. Westberry, N. Mahowald, D. M. Glover, and T. Takahashi (2009), Skill metrics for confronting global upper ocean ecosystem biogeochemistry models against field and remote sensing data, *J. Mar. Syst.*, *76*, 95–112, doi:10.1016/j.jmarsys.2008.05.015.

Feely, R. A., T. Takahashi, R. Wanninkhof, M. J. McPhaden, C. E. Cosca, S. C. Sutherland, and M.-E. Carr (2006), Decadal variability of the air-sea CO_2 fluxes in the equatorial Pacific Ocean, *J. Geophys. Res.*, *111*, C08S90, doi:10.1029/2005JC003129.

Friis, K., A. Körtzinger, J. Pätsch, and D. W. R. Wallace (2005), On the temporal increase of anthropogenic CO_2 in the subpolar North Atlantic, *Deep Sea Res., Part I*, *52*, 681–698, doi:10.1016/j.dsr.2004.11.017.

Gattuso, J. P., M. Frankignoulle, and R. Wollast (1998), Carbon and carbonate metabolism in coastal aquatic ecosystems, *Annu. Rev. Ecol. Syst.*, *29*, 405–434, doi:10.1146/annurev.ecolsys.29.1.405.

Gnanadesikan, A., M.-A. Pradal, and R. Abernathey (2015), Isopycnal mixing by mesoscale eddies significantly impacts oceanic anthropogenic carbon uptake, *Geophys. Res. Let.*, *42*, 2449–4255, doi:10.1002/2015GL064100.

González-Dávila, M., M. Santana-Casiano, and E. González-Dávila (2007), Interannual variability of the upper ocean carbon cycle in the north-east Atlantic Ocean, *Geophys. Res. Lett.*, *34*, L07608, doi:10.1029/2006GL028145.

Gouretski, V. V., and K. Jancke (2000), Systematic errors as the cause for an apparent deep water property variability: Global analysis of the WOCE and historical hydrographic data, *Prog. Oceanogr.*, *48*, 337–402, doi:10.1016/S0079-6611(00)00049-5.

Gruber, N. (1998), Anthropogenic CO2 in the Atlantic Ocean, *Global Biogeochem. Cycles*, *12*, 165–191.

Gruber, N., J. L. Sarmiento, and T. F. Stocker (1996), An improved method for detecting anthropogenic CO_2 in the oceans, *Global Biogeochem. Cycles*, *10*, 809–837.

Hood, E. M., L. Merlivat, and T. Johannessen (1999), Variations of fCO_2 and air-sea flux of CO_2 in the Greenland Sea gyre using high-frequency time series data from CARIOCA drift buoys, *J. Geophys. Res.*, *104*, 20,571–20,583, doi:10.1029/1999JC900130.

Hutchins, D. A., F.-X. Fe, Y. Zhang, M. E. Warner, Y. Feng, K. Portune, P. W. Bernhardt, and M. R. Mullholland (2007), CO_2 control of *Trichodesmium* N_2 fixation, photosynthesis, growth rates, and elemental ratios: Implications for past, present, and future ocean biogeochemistry, *Limnol. Oceanogr.*, *52*(4), 1293–1304.

Ito, T., M. Woloszyn, and M. Mazloff (2010), Anthropogenic carbon dioxide transport in the Southern Ocean driven by Ekman flow, *Nature*, *463*, 80–84, doi:10.1038/nature08687.

Jones, D. C., I. Takamitsu, Y. Takano, and W.-C. Hsu (2014), Spatial and seasonal variability of the air-sea equilibration timescale of carbon dioxide, *Global Biogeochem. Cycles*, *28*, 1163–1178, doi:10.1002/2014GB004813.

Joyce, T. M., Jr., A. Hernandez-Guerra, and W. M. Smethie (2001), Zonal circulation in the NW Atlantic and Caribbean from a meridional World Ocean Circulation experiment hydrographic section at 66.1W, *J. Geophys. Res.*, *106*, 22,095–22,113.

Key, R. M., A. Kozyr, C. L. Sabine, K. Lee, R. Wanninkhof, J. L. Bullister, R. A. Feely, F. J. Millero, C. Mordy, and T. H. Peng (2004), A global ocean carbon climatology: Results from Global Data Analysis Project (GLODAP), *Global Biogeochem. Cycles*, *18*, GB4031, doi:10.1029/2004GB002247.

Key, R. M., et al. (2010), The CARINA data synthesis project: Introduction and overview, *Earth Syst. Sci. Data*, *2*, 105–121, doi:10.5194/essd-2-105-2010.

Khatiwala, S., et al. (2013), Global ocean storage of anthropogenic carbon, *Biogeosciences*, *10*, 2169–2191.

Kleypas, J. A., R. W. Buddemeier, D. Archer, J. Gattuso, C. Langdon, and B. N. Opdyke (1999), Geochemical consequences of increased atmospheric carbon dioxide on coral reefs, *Science*, *284*, 118–120, doi:10.1126/science.284.5411.118.

Kurihara, H., and Y. Shirayama (2004), Effects of increased atmospheric CO_2 on sea urchin early development, *Mar. Ecol. Prog. Ser.*, *274*, 161–169.

Lachkar, Z., J. C. Orr, and J.-C. Dutay (2009), Seasonal and mesoscale variability of oceanic transport of anthropogenic CO_2, *Biogeosciences*, *6*, 2509–2523, doi:10.5194/bg-6-2509-2009.

Langdon, C., and M. Atkinson (2005), Effect of elevated pCO_2 on photosynthesis and calcification of corals and interactions with seasonal change in temperature/irradiance and nutrient enrichment, *J. Geophys. Res.*, *110*, C09S07, doi:10.1029/2004JC002576.

Langdon, C., T. Takahashi, C. Sweeney, D. Chipman, J. Goddard, F. Marubini, H. Acevec, H. Barnett, and M. J. Atkinson (2000), Effect of calcium carbonate saturation state on the calcification rate of an experimental coral reef, *Global Biogeochem. Cycles*, *14*, 639–654, doi:10.1029/1999GB001195.

Lauvset, S. K., and N. Gruber (2014), Long-term trends in surface ocean pH in the North Atlantic, *Mar. Chem.*, *162*(20), 71–76, doi:10.1016/j.marchem.2014.03.009.

Lee, K., et al. (2003), An updated anthropogenic CO_2 inventory in the Atlantic Ocean, *Global Biogeochem. Cycles*, *17*(4), 1116, doi:10.1029/2003GB002067.

Le Quéré, C., et al. (2015), Global carbon budget 2014, *Earth Syst. Sci. Data*, *7*, 47–85.

Levine, N. M., S. C. Doney, R. Wanninkhof, K. Lindsay, and I. Y. Fung (2008), The impact of ocean carbon system variability on the detection of temporal increases in anthropogenic CO_2, *J. Geophys. Res.*, *113*, C03019, doi:10.1029/2007JC004153.

Macdonald, A. M., M. O. Baringer, R. Wanninkhof, K. Lee, and D. W. R. Wallace (2003), A 1998–1992 comparison of inorganic carbon and its transport across 24.5°N in the Atlantic, *Deep Sea Res., Part II*, *50*, 3041–3064, doi:10.1016/j.dsr2.2003.07.009.

McDougall, T. J., and P. M. Barker (2011), *Getting Started With TEOS-10 and the Gibbs Seawater (GSW) Oceanographic Toolbox*, 28 pp., SCOR/IAPSO WG127.

McGrath, T., C. Kivimae, T. Tanhua, R. R. Cave, and E. McGovern (2012), Inorganic carbon and pH levels in the Rockall Trough 1991–2010, *Deep Sea Res., Part I*, *68*, 79–91.

Michaelidis, B., C. Ouzounis, A. Paleras, and H. O. Portner (2005), Effects of long-term moderate hypercapnia on acid-base balance and growth rate in marine mussels *Mytilus galloprovincialis*, *Mar. Ecol. Prog. Ser.*, *293*, 109–118.

Mikaloff Fletcher, S. E., et al. (2006), Inverse estimates of anthropogenic CO_2 uptake, transport, and storage by the ocean, *Global Biogeochem. Cycles*, *20*, GB2002, doi:10.1029/2005GB002530.

Millero, F. J. (1995), Thermodynamics of the carbon dioxide system in the Oceans, *Geochim. Cosmochim. Acta*, *59*(4), 661–677.

Millero, F. J. (2007), The marine inorganic carbon cycle, *Chem. Rev.*, *107*(2), 308–341.

Millero, F. J., T. B. Graham, F. Huang, H. Bustos-Serrano, and D. Pierrot (2006), Dissociation constants of carbonic acid in seawater as a function of salinity and temperature, *Mar. Chem.*, *100*, 80–94, doi:10.1016/j.marchem.2005.12.001.

Millero, F. J., R. Woosley, B. DiTrolio, and J. Waters (2009), The effect of ocean acidification on the speciation of metals in natural waters, *Oceanography*, *22*(4), 72–85.

Millero, F. J., J. Sharp, R. J. Woosley, C. Rodriguez, J. Paine, J. Levy, J. Williamson, J. Byrnes, and K. Mastropole (2014), Global Ocean Repeat Hydrography Study: pH and Total Alkalinity Measurements in the Atlantic Ocean A16 North and South Aug. 2014–Feb. 2014, Tech. Rep., Univ. of Miami, Miami, Fla.

Murata, A., Y. Kumamoto, K. Sasaki, and S. Watanabe (2008), Decadal increases of anthropogenic CO_2 in the subtropical South Atlantic Ocean along 30°S, *J. Geophys. Res.*, *113*, C06007, doi:10.1029/2007JC004424.

Palacios, S., and R. C. Zimmerman (2007), Response of eelgrass *Zostera marina* to CO_2 enrichment: Possible impacts of climate change and potential for remediation of coastal habitats, *Mar. Ecol. Prog. Ser.*, *344*, 1–13.

Patsavas, M. C., R. H. Byrne, R. Wanninkhof, R. A. Feely, and W. J. Cai (2015), Internal consistency of marine carbonate system measurements and assessments of aragonite saturation state: Insights from two U.S. coastal cruises, *Mar. Chem.*, *176*, 9–20, doi:10.1016/j.marchem.2015.06.022.

Pérez, F. F., M. Vázquez-Rodríguez, H. Mercier, A. Velo, P. Lherminier, and A. F. Ríos (2010), Trends of anthropogenic CO_2 storage in North Atlantic water masses, *Biogeosciences*, *7*, 1789–1807, doi:10.5194/bg-7-1789-2010.

Pérez, F. F., H. Mercier, M. Vázquez-Rodríguez, P. Lherminier, P. C. Pardo, G. Rosón, and A. F. Ríos (2013), Atlantic Ocean CO_2 uptake reduced by weakening of the meridional overturning circulation, *Nat. Geosci.*, *6*, 146–152, doi:10.1038/ngeo1680.

Plancherel, Y., K. B. Rodgers, R. M. Key, A. R. Jacobson, and J. L. Sarmiento (2013), Role of regression model selection and station distribution of the estimation of oceanic anthropogenic carbon change by eMLR, *Biogeosciences*, *10*, 4801–4831, doi:10.5194/bg-10-4801-2013.

Quay, P., R. Sonnerup, J. Stutsman, J. Maurer, A. Körtzing, X. A. Padin, and C. Robinson (2007), Anthropogenic CO_2 accumulation rates in the North Atlantic Ocean from changes in the $^{13}C/^{12}C$ of dissolved inorganic carbon, *Global Biogeochem. Cycles*, *21*, GB1009, doi:10.1029/2006GB002761.

Ríos, A. F., X. A. Álvarez-Salgado, F. F. Pérez, L. S. Bingler, and J. Arístegui (2003), Carbon dioxide along WOCE line A14: Water masses characterization and anthropogenic entry, *J. Geophys. Res.*, *108*(C4), 3123, doi:10.1029/2000JC000366.

Ríos, A. F., L. Resplandy, M. I. García-Ibáñez, N. M. Fajar, A. Velo, X. A. Padin, R. Wanninkhof, R. Steinfeldt, G. Rosón, and F. F. Pérez (2015), Decadal acidification in the water masses of the Atlantic Ocean, *Proc. Natl. Acad. Sci. U.S.A.*, *112*(32), 9950–9955, doi:10.1073/pnas.1504613112.

Rost, B., and U. Riebesell (2004), Coccolithophores and the biological pump: Responses to environmental changes, in *Coccolithophores—From Molecular Processes to Global Impact*, edited by H. R. Thierstein and J. R. Young, pp. 76–99, Springer, Berlin.

Sabine, C. L., and T. Tanhua (2010), Estimation of anthropogenic CO_2 inventories in the ocean, *Annu. Rev. Mar. Sci.*, *2*, 175–198, doi:10.1146/annurev-marine-120308-080947.

Sabine, C. L., R. A. Feely, R. M. Key, J. L. Bullister, F. J. Millero, K. Lee, T.-H. Peng, B. Tilbrook, T. Ono, and C. S. Wong (2002), Distribution of anthropogenic CO_2 in the Pacific Ocean, *Global Biogeochem. Cycles*, *16*(4), 1083, doi:10.1029/2001GB001639.

Sabine, C. L., et al. (2004), The oceanic sink for anthropogenic CO_2, *Science*, *305*, 367–371, doi:10.1126/science.1097403.

Sabine, C. L., R. A. Feely, F. J. Millero, A. G. Dickson, C. Langdon, S. Mecking, and D. Greeley (2008), Decadal changes in Pacific carbon, *J. Geophys. Res.*, *113*, C07021, doi:10.1029/2007JC004577.

Sarmiento, J. L., J. C. Orr, and U. Siegenthaler (1992), A perturbation simulation of CO_2 uptake in the ocean general circulation model, *J. Geophys. Res.*, *97*, 3621–3645, doi:10.1029/91JC02849.

Srokosz, M. A., and H. L. Bryden (2015), Observing the Atlantic Meridional Overturning Circulation yields a decade of inevitable surprises, *Science*, *348*(6241), doi:10.1126/science.1255575.

Steinfeldt, R., M. Rhein, J. L. Bullister, and T. Tanhua (2009), Inventory changes in anthropogenic carbon from 1997–2003 in the Atlantic Ocean between 20°S and 65°N, *Global Biogeochem. Cycles*, *23*, GB3010, doi:10.1029/2008GB003311.

Stocker, T. F., D. Qin, G.-K. Plattner, M. Tignor, S. K. Allen, J. Boschung, A. Nauels, Y. Xia, V. Bex, and P. M. Midgley (Eds) (2013), *Climate Change 2013: The Physical Science Basis. Contribution of Working Group I to the Fifth Assessment Report of the Intergovernmental Panel on Climate Change*, Cambridge Univ. Press, Cambridge, U. K.

Tanhua, T., A. Biastoch, A. Kortzinger, H. Luger, C. Boning, and D. W. R. Wallace (2006), Changes of anthropogenic CO_2 and CFCs in the North Atlantic between 1981 and 2004, *Global Biogeochem. Cycles*, *20*, GB4017, doi:10.1029/2006GB002695.

Thacker, W. C. (2012), Regression-based estimates of the rate of accumulation of anthropogenic CO_2 in the ocean: A fresh look, *Mar. Chem.*, *132–133*, 44–55, doi:10.1016/j.marchem.2012.02.004.

Uppstrom, L. R. (1974), The boron/chlorinity ratio of deep-sea water from the Pacific Ocean, *Deep Sea Res.*, *21*(2), 161–162.

U.S. Department of Energy (1994), *Handbook of Methods for the Analysis of the Various Parameters of the Carbon Dioxide System in Sea Water, Version 2*, *Rep. ORNL/CDIAC-17*, Oak Ridge Natl. Lab., Oak Ridge, Tenn.

Van Heuven, S., D. Pierrot, E. Lewis, and D. W. R. Wallace (2009), *MATLAB Program Developed for CO_2 System Calculations*, U.S. Dep. of Energy, Carbon Dioxide Inf. Anal. Center, Oak Ridge Natl. Lab., Oak Ridge, Tenn.

Vázquez-Rodríguez, M., F. F. Pérez, A. Velo, A. F. Ríos, and H. Mercier (2012), Observed acidification trends in North Atlantic water masses, *Biogeosciences*, *9*, 5217–5230.

Wallace, D. W. R. (1995), Monitoring global ocean carbon inventories, OOSDP Background Rep. 5, Tex. Agric. and Mech. Univ., College Station, Tex.

Wanninkhof, R., T.-H. Peng, B. Huss, C. L. Sabine, and K. Lee (2003), Comparison of inorganic carbon system parameters measured in the Atlantic Ocean from 1990 to 1998 and recommended adjustments, *Rep*. ORNL/CDIAC-140, Oak Ridge Natl. Lab., Oak Ridge, Tenn.

Wanninkhof, R., S. C. Doney, J. L. Bullister, N. M. Levine, M. Warner, and N. Gruber (2010), Detecting anthropogenic CO_2 changes in the interior Atlantic Ocean between 1989 and 2005, *J. Geophys. Res.*, *115*, C11028, doi:10.1029/2010JC006251.

Wanninkhof, R., G.-H. Park, T. Takahashi, R. A. Feely, J. L. Bullister, and S. C. Doney (2013), Changes in deep-water CO_2 concentrations over the last several decades determined from discrete pCO_2 measurements, *Deep Sea Res., Part I*, *74*, 48–63.

Watanabe, Y. W., T. Ono, and A. Shimamoto (2000), Increase in the uptake rate of ocean anthropogenic carbon in the North Pacific determined by CFC ages, *Mar. Chem.*, *72*, 297–315, doi:10.1016/S0304-4203(00)00087-6.

Waters, J. F., F. J. Millero, and C. L. Sabine (2011), Changes in South Pacific anthropogenic carbon, *Global Biogeochem. Cycles*, *25*, GB4011, doi:10.1029/2010GB003988.

Williams, N. L., R. A. Feely, C. L. Sabine, A. G. Dickson, J. H. Swift, L. D. Talley, and J. L. Russell (2015), Quantifying anthropogenic carbon inventory changes in the Pacific sector of the Southern Ocean, *Mar. Chem.*, *174*, 147–160, doi:10.1016/j.marchem.2015.06.15.

World Ocean Circulation Experiment (1994), *WOCE Operations Manual*, *Section 3.1: WOCE Hydrographic Program*, 144 pp., WOCE, Woods Hole, Mass.

Yao, W., X. Liu, and R. H. Byrne (2007), Impurities in indicators used for spectrophotometric seawater pH measurements: Assessment and remedies, *Mar. Chem.*, *107*(2), 167–172, doi:10.1016/j.marchem.2007.06.012.

Zhao, J., and W. Johns (2014), Wind-forced variability of the Atlantic meridional overturning circulation at 26.5°N, *J. Geophys. Res. Oceans*, *119*, 2403–2419, doi:10.1002/2013JC009407.

Zondervan, I. (2007), The effects of light, macronutrients, trace metals and CO_2 on the production of calcium carbonate and organic carbon in coccolithophores—A review, *Deep Sea Res., Part II*, *54*, 521–537.

Zunino, P., F. F. Pérez, N. M. Noelia, E. F. Guallart, A. F. Ríos, and J. L. Pelegrí (2015), Transports and budgets of anthropogenic CO2 in the tropical North Atlantic in 1992–1993 and 2010–2011, *Global Biogeochem. Cycles*, *29*, 1075–1091, doi:10.1002/2014GB005075.